

# FINAL PUBLISHABLE JRP REPORT

|  |  |                         |
|--|--|-------------------------|
| JRP-Contract number  | SIB59  |                         |
| JRP short name   | Q-WAVE   |                         |
| JRP full title   | A quantum standard for sampled electrical measurements |                         |
| Version numbers of latest contracted Annex Ia and Annex Ib against which the assessment will be made | Annex Ia:  | V1.0                    |
|  | Annex Ib:  | V1.0                    |
| Period covered (dates)   | From 1 June 2013                                       | To 31 May 2016          |
| JRP-Coordinator  |  |                         |
| Name, title, organisation  | Dr. Johannes Kohlmann, PTB                             |                         |
| Tel:   | ++ 49 (0) 531 592 2133                                 |                         |
| Email:   | johannes.kohlmann@ptb.de                               |                         |
| JRP website address  | www.ptb.de/emrp/qwave.html                             |                         |
| Other JRP-Partners   |  |                         |
| Short name, country  | CEM, Spain   | NPL, United Kingdom     |
|  | CMI, Czech Republic                                    | SIQ, Slovenia           |
|  | INRIM, Italy   | SP, Sweden              |
|  | JV, Norway   | TUBITAK, Turkey         |
|  | METAS, Switzerland                                     | VSL, Netherlands        |
|  | VTT, Finland   |                         |
| REG-Researcher (associated Home Organisation)  |  |                         |
| Researcher name, title   | Per Ohlckers, Professor                                | Start date: 1 Nov. 2013 |
| (Home organisation Short name, country)  | HBV, Norway  | Duration: 26 months     |

**Report Status: PU Public**



## TABLE OF CONTENTS

|          |   |           |
|----------|---|-----------|
| <b>1</b> | <b>Executive Summary .....</b>  | <b>3</b>  |
| <b>2</b> | <b>Project context, rationale and objectives .....</b>                                      | <b>4</b>  |
| <b>3</b> | <b>Research results.....</b>  | <b>7</b>  |
| 3.1      | Measurement system based on the Josephson effect.....                                       | 7         |
| 3.1.1    | Josephson arrays .....  | 7         |
| 3.1.1.1  | Improved pulse-driven arrays: design and fabrication technology .....                       | 8         |
| 3.1.1.2  | Pulse-driven Josephson arrays achieve 1 V .....   | 9         |
| 3.1.1.3  | Operation of pulse-driven Josephson arrays in a cryo-cooler.....                            | 9         |
| 3.1.2    | Low temperature photodiodes.....  | 10        |
| 3.1.3    | Optoelectronic pulse generation system .....  | 11        |
| 3.1.4    | Delta Sigma electronics.....  | 12        |
| 3.1.5    | Conclusion.....   | 14        |
| 3.2      | Dissemination methods .....   | 14        |
| 3.2.1    | Quantum-based characterisation of ADC .....   | 14        |
| 3.2.1.1  | Josephson mercury wetted relay step generator .....   | 14        |
| 3.2.1.2  | Delta-sigma PJVS .....  | 15        |
| 3.2.1.3  | PJVS test bench .....   | 16        |
| 3.2.1.4  | Pulse-driven Josephson arrays .....   | 17        |
| 3.2.2    | Development and use of DAC-based AC voltage reference sources .....                         | 19        |
| 3.2.2.1  | High-stability arbitrary waveform generator DualDAC .....                                   | 19        |
| 3.2.2.2  | Wideband DAC-based synthesiser .....  | 21        |
| 3.2.3    | Comparison and validation of sampling methods .....   | 21        |
| 3.2.3.1  | Comparing sampling and thermal techniques .....   | 22        |
| 3.2.3.2  | Inter-comparison.....   | 22        |
| 3.2.4    | Conclusion.....   | 23        |
| 3.3      | Digital signal processing techniques .....  | 23        |
| 3.3.1    | Improved digital signal processing techniques.....  | 23        |
| 3.3.1.1  | Improved sampled signal estimation for harmonically distorted signals .....                 | 23        |
| 3.3.1.2  | Jitter and noise of 3458A sampling DMM modeled, measured and explained .....                | 24        |
| 3.3.1.3  | Estimation of sampled arbitrary signal power .....  | 25        |
| 3.3.2    | Contribution of signal processing on measurement uncertainty .....                          | 25        |
| 3.3.2.1  | Software Toolbox.....   | 26        |
| 3.3.2.2  | Cable resonance phenomena for pulse-driven Josephson source explained .....                 | 27        |
| 3.3.3    | Characterisation of converters .....  | 28        |
| 3.3.3.1  | List of analogue-to-digital converter parameters that require improved characterisation ... | 28        |
| 3.3.3.2  | High accuracy parameters that require improved characterisation.....                        | 28        |
| 3.3.3.3  | Procedure for improved characterisation of ADC.....   | 28        |
| 3.3.4    | Conclusion.....   | 29        |
| <b>4</b> | <b>Actual and potential impact .....</b>  | <b>29</b> |
| 4.1      | Dissemination of results .....  | 30        |
| 4.2      | Impact on the metrological and scientific communities .....                                 | 30        |
| 4.3      | Impact on standardisation .....   | 31        |
| 4.4      | Early impact on end users.....  | 31        |
| 4.5      | Potential future impact.....  | 31        |
| <b>5</b> | <b>Website address and contact details .....</b>  | <b>32</b> |
| <b>6</b> | <b>List of publications.....</b>  | <b>32</b> |



## 1 Executive Summary

### Introduction

Digital metrology is now the method of choice in the instrumentation sector, therefore the performance of electrical sensors depends on the conversion of analogue measurements to digital signals, and vice versa. This conversion process relies on sampling the voltage signal and converting it to a frequency, which is relatively straightforward for direct current signals but harder for alternating current (AC). Recent progress in the semiconductor industry, and particularly in precision integrated circuits, has exposed the need for higher sampling rates and greater accuracy for high-precision voltage measurements for analogue-to-digital converters (ADC) and digital-to-analogue converters (DAC).

The Josephson effect, which links frequency and voltage very accurately, is well established as a primary standard for DC voltage. This project investigated extending the use of the Josephson effect to AC voltage measurements, so that the latest generation of ADC can be calibrated. The progress included proof of concept, development of the technology and sampling measurement procedures, as well as direct traceability for these measurements.

### The Problem

Digital metrology is a large and growing field used in all industrial sectors from white goods to sophisticated medical instruments and advanced electronics. It is now the method of choice in the instrumentation sector, with sensing and measurement becoming increasingly dependent on analogue-to-digital conversion of sampled measurements. An analogue voltage or current from a sensor is converted into a digital quantity using an ADC at the earliest opportunity. Once the electrical signal has been digitised, quantities such as the basic root mean square (RMS) value, peak value, crest factor and harmonic content can all be calculated directly, rather than each quantity requiring specific measurement and calibration. Recent industrial R&D in precision integrated circuits and measurement equipment has brought about a step change in the sampling rates and potential accuracy available. However, the methods for disseminating the SI volt for non-stationary or alternating waveforms had not been keeping pace with requirements.

### The Solution

The project addressed the lack of instrumentation and knowledge for providing direct and efficient traceability to the SI volt for ADCs and DACs operating in the DC to 10 MHz range i.e. to provide direct traceability for sampled electrical measurements to quantum voltage standards in terms of the Josephson effect. It then looked at dissemination methods using state of the art instruments, and finally examined ways of coping with the large quantity of data being produced by these quicker signal processing techniques to make best use of them.

### Impact

The project proved that Josephson-based systems can be used to calibrate ADCs at higher voltages and faster rates than previously possible. The project significantly improved the instrumentation and knowledge for providing direct and efficient traceability to the SI representation of the volt, in terms of the Josephson effect for AC waveforms including sampling measurements.



## 2 Project context, rationale and objectives

This project addressed the lack of instrumentation and knowledge for providing direct and efficient traceability to the SI volt in terms of the Josephson effect for ADC and DAC operating up to the MHz range.

### Project context and rationale

Modern instrumentation (e.g. balances, instrumentation for measurement of all electrical quantities, oscilloscopes, spectrum analysers, etc.) relies heavily on digital techniques using digital circuits containing ADCs and DACs. In most cases, an analogue voltage or current from a sensor is converted into a digital quantity using an ADC at the earliest opportunity in this instrumentation normally used in industry, research and calibration laboratories. A key benefit of the digital techniques is that once the electrical signal has been digitised, quantities such as the RMS value, peak value, crest factor and harmonic content can all be calculated from one dataset whereas previously, each quantity required a special instrument feature or range and each of these ranges had to be separately calibrated. Digital signal processing can also be used to perform functions from simple operations such as scaling and filtering to more complex tasks such as spectral analysis, curve fitting and feature extraction. The reverse is also true in that an instrument can generate a voltage or current as a series of discrete levels using a digital-to-analogue converter (DAC). With access to purpose built digital signal processing devices, instrument designers and scientific researchers can implement the required features more cost effectively than in analogue circuits and benefit from a straightforward upgrade path through improvements to software or firmware. The primary electrical quantity being measured is therefore a series of voltage samples. These may be of stationary value with random noise or be varying in a repetitive or arbitrary manner. Since signal processing algorithms can be constructed with predictable and calculable numerical accuracy, the traceability of the voltage samples is a critical component in the uncertainty budget.

The performance of ADCs and DACs is described in a number of ways and it is the role of standards bodies to unify this. Traceability of the final system can only be ensured with a detailed knowledge of the converter characteristics and the way in which they are specified and measured. In many cases, relative rather than absolute measurements are required (e.g. relative level of harmonic distortion in a waveform rather than the exact amplitude of the fundamental). A Josephson voltage standard is ideally placed to provide both relative and absolute measurements, as it is a quantum standard of voltage and a fundamentally linear device for the measurement of relative parameters.

Routine uses of the Josephson effect as a quantum standard of voltage have been limited to DC voltages for a long time. Traceability for AC voltages is mainly provided using thermal transfer devices which equate the electrical heating power of a direct current (DC) and an alternating current (AC) input. After many years of development, these thermal transfer devices can deliver a few parts in  $10^6$  accuracies over a wide range of frequencies and voltages. However, they are fragile and need considerable care in order to realise their best performance. Furthermore, as they operate on the square of the voltage input, they can only give information on the total sum of squares of the voltages applied but not on the harmonic content of the waveform being measured. Thus they are normally used to provide traceability for repetitive waveforms of constant amplitude and low harmonic content. Traceability from National Metrology Institutes (NMIs) to the next level of users as high-level calibration laboratories usually involves the calibration of precision sources of alternating voltage, known as calibrators, using a calibrated thermal transfer device and a DC voltage reference. This has to be done at many frequencies and voltages and is a time consuming process. A calibrator can only typically hold the transferred value to 50 parts in  $10^6$  or worse and the measured quantity is still a basic root mean square (RMS) amplitude.

In addition, the rapid progress of semiconductor industry offering sophisticated ADCs and DACs with increasing sampling rates and accuracy causes an increasing demand for a significant improvement of high-precision voltage measurements including traceability to the SI volt. The traceability to the SI for non-stationary waveforms, in particular, is not keeping pace with the evolution in digital electrical metrology. A key aspect of the traceability of a measurement system for dynamic quantities is the performance of the electronic amplifier and ADC. Currently, no direct traceability for this electrical measurement exists. For many waveforms a single frequency is not an adequate representation of the quantity being measured and there is no traceability for arbitrary waveforms with sufficiently low uncertainty.



This research project addressed the above mentioned problems and gave the first steps to bring about a fundamental change to the way in which the volt is disseminated in the SI for AC waveforms. In addition, as direct traceability to the quantum standard of voltage based on the Josephson effect is provided for sampled electrical measurements, the project started to establishing a new infrastructure for traceability of voltage waveforms directly to the SI representation of the volt in terms of the Josephson effect. A main part of the work was focused on dissemination methods based on state of the art instrumentation and converters including techniques for both repetitive and single shot waveforms, in order to bridge the gap between quantum-based waveform standards and the test and calibration needs from semiconductor industry and instrumentation manufacturers. Existing calibrators based on electronic devices for dissemination played an important role to achieve the goals. First, these calibrators required adaption, before they could be used for investigations, measurements, and comparisons.

The quantum standard of voltage is based on the Josephson effect, which relates voltage to frequency in so-called Josephson junctions being composed of two weakly coupled superconductors. More than 50 voltage standards based on the Josephson effect are in operation around the world, some of them in top level industrial laboratories; most of these standards are suited for DC applications. The Josephson effect provides a quantum standard because the conversion factor between voltage and frequency depends only on two fundamental constants, the elementary charge ( $e$ ) and the Planck constant ( $h$ ). Thus with access to a frequency reference, the unit of voltage, the Volt (V), can be reproduced anywhere with an accuracy (for practical purposes) limited only by the traceability of the frequency. To date, the metrology community has operated with an internationally agreed or conventional value of the conversion factor, known as the Josephson constant,  $K_J$ , where  $K_J = 2e/h$ , set in 1990 such that  $K_{J-90} = 483\,597.9$  GHz/V. Currently, this maintained unit of voltage has an uncertainty in the SI. However, when the forthcoming redefinition of the SI takes place,  $h$  and  $e$  are expected to be given exact values allowing this quantum standard of voltage to be realised directly in the SI.

The work of this project was partly based on outcomes of former research projects i) some developments of AC Josephson voltage standards as well as their initial use and application were achieved in the iMERA-Plus project JoSy (Next generation of quantum voltage systems for wide range applications), 2008 – 2011, ii) some fundamental mathematical approaches for determining the uncertainty propagation between time- and frequency domains for large sets of sampled data were investigated in the EMRP project ‘Ultrafast’ (Metrology for ultrafast electronics and high-speed communications), 2011 – 2014 and iii) first developments and investigations of pulse-driven AC Josephson voltage standard were performed in the JAWS project of the Framework V programme (Josephson Arbitrary Waveform Synthesiser: realisation of a quantum standard for AC voltage), 2001 – 2004. .

#### AC Josephson voltage standards: a brief introduction

A major part of this project was related to using Josephson voltage standards for AC applications. This subsection briefly summarises some fundamentals of AC Josephson voltage standards, as this background is required for understanding major parts of this project including the objectives and to evaluate the results of the R&D work described in chapter 3.

The development of AC Josephson voltage standards has been carried out over nearly two decades and has been focused on two different approaches both based on overdamped Josephson junctions. The first approach consists of Josephson junction series arrays (which are operated by a sinusoidal microwave drive (cf. <sup>1</sup>, <sup>2</sup>)), in which the number of junctions per segment follows a binary sequence. The second approach is based on Josephson junction series arrays that are biased with a high-speed digital sequence of short current pulses (cf. <sup>3</sup>, <sup>4</sup>).

As these two approaches are based on different operation principles, they show different advantages and limitations. A binary-divided series array is operated as a multi-bit DAC; so it allows a sine wave to be synthesized as a step-approximated waveform, but this waveform contains many higher harmonics. In

<sup>1</sup> J. Lee, R. Behr, L. Palafox, A. Katkov, M. Schubert, M. Starkloff, A.C. Böck, *An ac quantum voltmeter based on a 10 V programmable Josephson array*, Metrologia **50** (2013) 612 – 622.

<sup>2</sup> A. Rüfenacht, C.A. Burroughs, P.D. Dresselhaus, S.P. Benz, *Differential sampling measurement of a 7 V rms sine wave with a programmable Josephson voltage standard*, IEEE Trans. Instrum. Meas. **62** (2013) 1587 – 1593.

<sup>3</sup> R. Behr, O. Kieler, J. Kohlmann, F. Müller und L. Palafox, *Development and metrological applications of Josephson arrays at PTB*, Meas. Sci. Technol. **23** (2012) 124002 (19 pp).

<sup>4</sup> S.P. Benz, P.D. Dresselhaus, A. Rüfenacht, N.F. Bergren, J.R. Kinard, R.P. Landim, *Progress toward a 1 V pulse-driven AC Josephson voltage standard*, IEEE Trans. Instrum. Meas. **58** (2009) 838 – 843.



addition, the transients between the constant-voltage steps significantly contribute to the uncertainties. Therefore, binary-divided arrays are mainly used for applications at DC and moderate frequencies from a few Hz to about 3 kHz; best results are often achieved in combination with sampling methods. Series arrays for output voltages of 10 V are available.<sup>1, 2</sup> On the other hand, pulse-driven arrays enable spectrally pure arbitrary waveforms to be synthesized. The train of short current pulses is typically provided by a commercial pulse pattern generator (PPG) with a maximum pulse repetition frequency of about 15 GHz. Because of the complex pulse drive, the output voltage was limited to RMS values of about 300 mV at most for a long time, as only two series arrays could be simultaneously operated.<sup>3, 4</sup> Therefore, a major goal of this project and other research activities was to increase the output voltage of pulse-driven Josephson systems.

To reach output voltages of 1 V or 10 V, Josephson arrays containing tens of thousands junctions are required. An advanced and reliable fabrication technology is a major prerequisite for the successful development of these highly integrated Josephson arrays. The most reliable technology is presently based on SNS-like Josephson junctions that contain a thin barrier made of highly resistive, amorphous  $Nb_xSi_{1-x}$  (S: Superconductor, N: Normal metal).<sup>1-4</sup>

### Objectives

This project aimed to provide direct and efficient traceability to the SI volt for precision devices generating or measuring arbitrary waves at frequencies up to 10 MHz, i.e. to provide direct traceability for sampled electrical measurements to quantum voltage standards. Therefore, this project addressed three scientific and technical objectives to:

1. Realise a **measurement system based on the Josephson effect** for the dynamic calibration of analogue-to-digital converters.
2. Establish **dissemination methods** based on the state of the art instrumentation and converters, including techniques for both repetitive and single shot waveforms.
3. Improve **digital signal processing techniques** and to evaluate their contribution to the measurement uncertainty.

### 3 Research results

This section summarises the research undertaken and the results and conclusions of that research. The three sub-sections are dedicated to addressing the three scientific and technical objectives, namely the Josephson ADC, dissemination methods, and digital signal processing techniques.

#### 3.1 Measurement system based on the Josephson effect

The development of a measurement system based on the Josephson effect for the dynamic calibration of ADCs and DACs, the Josephson ADC, was carried out because this system aimed to provide direct and efficient traceability to the SI volt required for the dissemination methods. This quantum-based ADC was planned to include Josephson arrays biased by low-temperature photodiodes, an optoelectronic pulse drive and delta sigma electronics. A schematic diagram of the system is given in Figure 1.1. The details of the components are described below as well as details of the results obtained when characterising various parts of the system. The first part of this work summarises the development of Josephson series arrays (section 3.1.1) and the second part is focused on the photodiodes (section 3.1.2). As a third activity, an optoelectronic pulse generation system has been developed (section 3.1.3). In the fourth part, the development of the Sigma-Delta electronics is described (section 3.1.4).

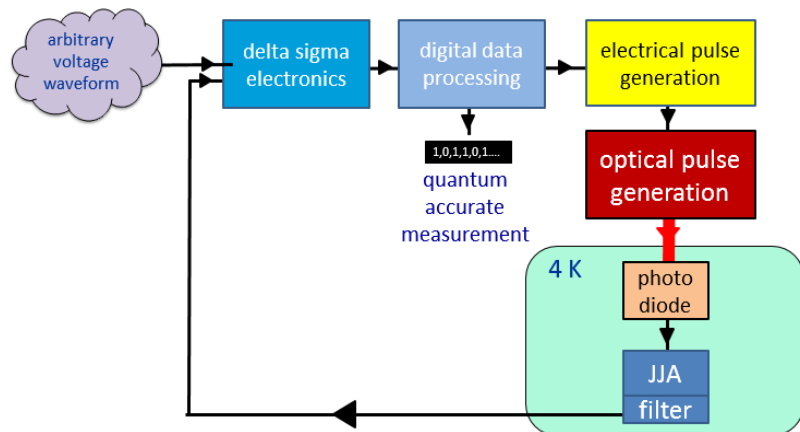


**Figure 1.1:** A schematic diagram of the Josephson ADC. An arbitrary voltage waveform is compared to the output of a Josephson junction array (JJA) using delta sigma electronics. This results in a delta sigma code which, after filtering, provides a quantum accurate representation of the input waveform. The delta sigma code is sent to an electrical pulse generation system that generates GHz rate pulses suitable to drive the Josephson array. Optoelectronic components are used to convert the pulses into optical pulses. These pulses drive a photodiode, which may be mounted at low temperature and used to drive the array. This optical drive has the advantage of allowing several arrays to be connected in series, since the drive system is electrically isolated from the array.

Besides the novel system, a system based on series arrays of Josephson junctions operated by a commercial PPG has been also investigated especially in view of increasing the output voltage. This system has been used as a quantum voltage standard for different applications related to dissemination methods (section 3.2.1.4).

This part of the project benefited greatly from the collaboration of the partners who brought complimentary expertise to the project. PTB developed the Josephson arrays, JV and HBV developed the low temperature photodiodes, NPL developed delta sigma electronics and an optoelectronic system and VSL developed delta sigma electronics. The various components described below had to be integrated to form the final system.

#### 3.1.1 Josephson arrays

The series arrays of Josephson junctions are a main component of the quantum-based ADC. Their operation by optoelectronics required the adjustment of their characteristic parameters for an optimised operation by optical pulses. In addition, the fabrication technology was improved to increase the number of junctions in a single array and thus the output voltage. Besides the use for the Josephson ADC, these devices have been operated as quantum voltage standard for different dissemination methods (section 3.2).

Different test arrays were designed and developed as the first step of these activities. The designs consist of arrays with four different numbers of Josephson junctions ranging from a single junction to up to 5,000 junctions and three junction sizes between about  $12 \mu\text{m}^2$  and  $50 \mu\text{m}^2$  resulting in different critical currents. These test arrays were designed, fabricated and characterised at PTB; and several arrays were distributed to project partners.

**3.1.1.1 Improved pulse-driven arrays: design and fabrication technology**

An important task on the development of the Josephson ADC was the increase of the output voltage delivered by a single pulse-driven array. To reach this goal, improvements on both the design and the technology were required. The RMS output voltage of typical arrays used at the beginning of the project was below 100 mV. The arrays consist of SNS junctions based on a NbSi normal metal barrier deposited in a co-sputter process. The first step of the development was to increase the typical RMS voltage above 100 mV. The design of the arrays was further improved and arrays were fabricated at PTB using double-stacked Josephson junctions. These arrays delivered RMS voltages up to nearly 120 mV.

Due to the excellent deposition conditions for the NbSi barrier junctions, the spread of the characteristic parameters of the Josephson junctions is extremely low. Triple-stacked junctions (as shown in Figure 1.2) with 8 layers deposited *in-situ* were successfully fabricated subsequently. Due to the small parameter spread in the critical current density, large series arrays of stacked junctions showed wide operation margins under pulse drive. Arrays with triple-stacked Josephson junctions were characterised at PTB. Up to 9,000 Josephson junctions were integrated into a single array allowing RMS output voltages of 178 mV (peak voltage of 251 mV). This result is an important step in increasing the output voltage of pulse-driven Josephson systems. Figure 1.3 shows a picture of a Josephson Arbitrary Waveform Synthesiser (pulse-driven Josephson voltage standard) (JAWS) chip mounted onto a special chip carrier (upper left) and three scanning electron microscope pictures of an array and some details of the Josephson junctions and on-chip filter structures. Some selected arrays were delivered to the project partners INRIM, JV, NPL, and VSL.

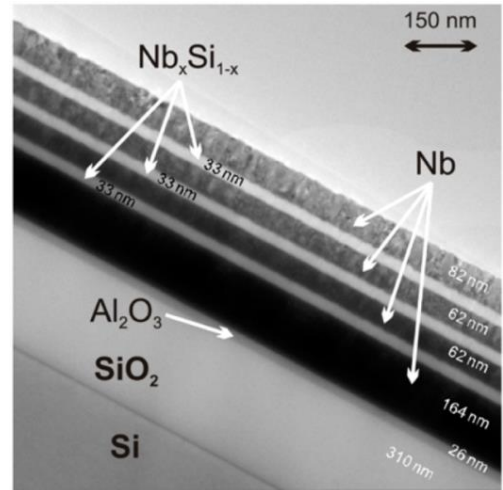


**Figure 1.2:** Transmission electron microscope picture of a triple-stacked Josephson junction with NbSi barrier for pulse-driven Josephson arrays. The thickness of each barrier layer is 33 nm.

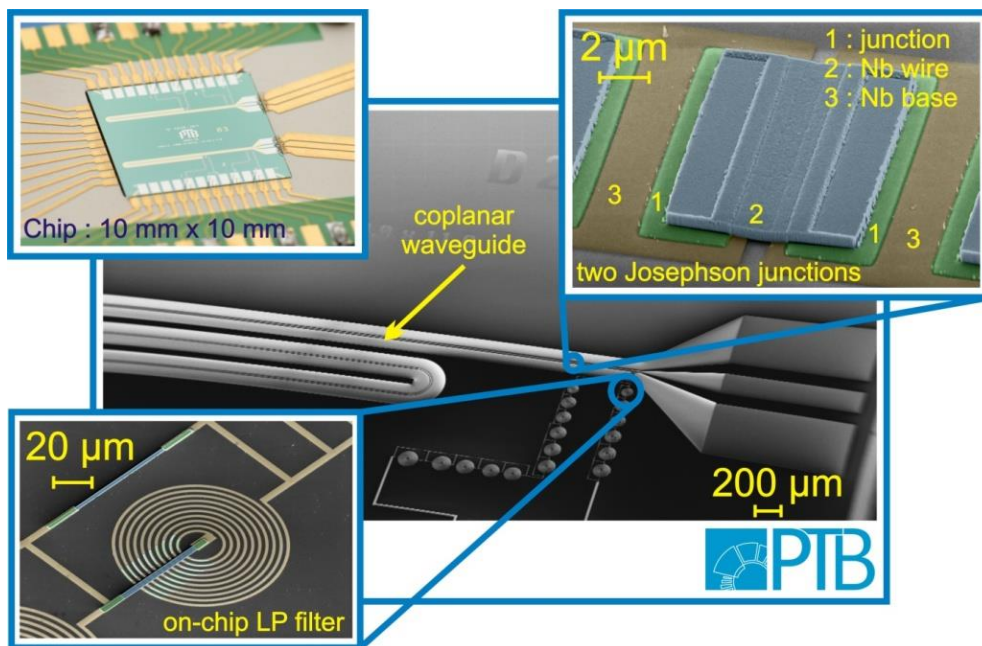


**Figure 1.3:** Photo (upper left) and scanning electron microscope pictures of some details of a typical pulse-driven Josephson series array embedded into the middle of a 50 Ω coplanar waveguide transmission line (CPW).

### 3.1.1.2 Pulse-driven Josephson arrays achieve 1 V

As Josephson systems based on pulse-driven junctions operated by a commercial pulse pattern generator have an outstanding relevance as quantum voltage standards, different developments have been performed in this area. The development of Josephson arrays delivering RMS voltages up to 178 mV is an important step in the development of a 1 V pulse-driven system by operation of some arrays simultaneously.

While only two arrays could be operated simultaneously by typical pulse pattern generators, an improved prototype 8-channel pulse pattern generator (BPG 30G-TER, Sympuls) delivering ternary pulses allowed the operation of up to eight arrays. Using a new sample holder, eight arrays could be really operated simultaneously; after some tests, a major breakthrough was achieved at PTB by demonstrating 1 V waveforms with eight arrays containing 63,000  $\text{Nb}_x\text{Si}_{1-x}$  barrier junctions in total [1]. As an example, Figure 1.4 shows the frequency spectrum and time domain signal of a synthesised sine waveform with a signal frequency of 250 Hz. Results showed that higher harmonics are suppressed by more than 120 dBc and the noise floor is suppressed by even 140 dBc. The current operation margins are 0.3 mA and the remaining higher harmonics are most likely related to cross-talk in the cryoprobe.

Figure 1.5 shows a photo of the 1 V measurement setup. It contains a new 8-channel cryoprobe and an 8-channel compensation electronics assembled at PTB. The 1 V system is a major achievements of this project, as this voltage will enable a lot of applications in AC metrology in the future. A direct comparison at PTB with the AC quantum voltmeter demonstrated an excellent agreement between the two quantum standards (cf. section 3.2.1.4).

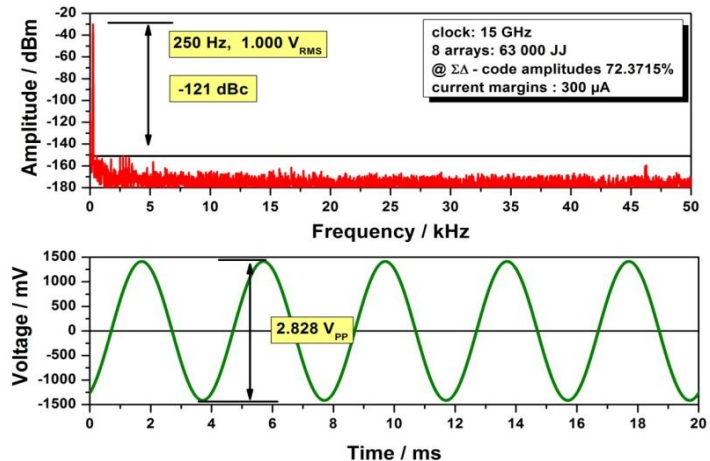


**Figure 1.4:** Frequency spectrum (top) and time domain signal (bottom) of a synthesised sine wave with an RMS output voltage of 1 V at a frequency of 250 Hz using eight Josephson arrays consisting of 63,000 Josephson junctions in total. Higher harmonics are suppressed by more than 120 dB.

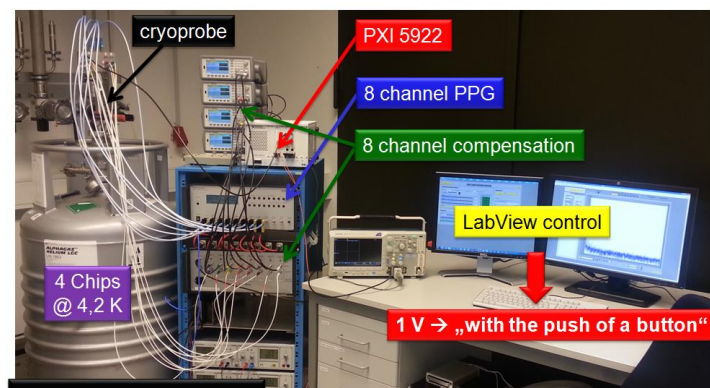


**Figure 1.5:** Photo of the 1 V measurement setup at PTB. Main components are marked.

### 3.1.1.3 Operation of pulse-driven Josephson arrays in a cryo-cooler

Operation of Josephson arrays in a cryo-cooler have been investigated and tested, as cryo-coolers offer two important advantages. First, in the short term, cryo-coolers enable rather short connections between the array at low temperatures and the devices under test at room temperature, which results in significantly improved accuracy at frequencies above 100 kHz. Secondly, in the long term, they enable a user-friendly operation of quantum voltage standards by avoiding the use of liquid helium. Therefore, some fundamental investigations and tests with cryo-coolers have been performed in the framework of this project.

At INRIM a cryo-cooler setup was established for operation of pulse-driven Josephson arrays delivered by PTB. This work was focused on an optimised setup including short cables, adapted high-frequency lines and improved thermal connection between cold head and Josephson array. Figure 1.6 shows the frequency spectrum of a synthesised sinusoidal waveform at a frequency of 1250 Hz, where higher harmonics are suppressed by more than 80 dBc.

Additional investigations were performed at PTB, where pulse-driven arrays were operated in a commercial pulse tube cryo-cooler. Bipolar waveforms were synthesized and pure spectra and stable operation margins were demonstrated up to 5.6 K [2].

### 3.1.2 Low temperature photodiodes

As part of the optoelectronics, photodiodes from Albis Optoelectronics were selected, based on the availability of bare dies with high speed up to 20 GHz. The model PDCS20T was tested first. These diodes have a simple structure and a small aperture of about 20  $\mu\text{m}$ , so the alignment to a fibre cable with a core diameter of 9  $\mu\text{m}$  is a tough challenge. Initial trials were based on gluing the diodes to a silicon wafer with laser etched grooves and thermally evaporated metal contacts. These experiments resulted in good alignment at room temperature, and a DC response of about 10 - 12 mA, but a stable alignment was difficult to achieve. The size of the diode is 500  $\mu\text{m}$  x 500  $\mu\text{m}$  with bonding pads of 70  $\mu\text{m}$  and 150  $\mu\text{m}$ . A test structure was made, where mechanical alignment was provided by flip-chip bonding the diode to a Si substrate, with a chemically etched hole centred on the aperture of the diode. These structures provided an unstable alignment, as the fibre cable could touch the edged of the hole, thereby diverting the laser beam. A second problem was related to the gluing of the fibre, which often led to the glue covering the lens. Some stable structures were tested at room temperature with good results. The DC response was around 23 mA for many samples, but during cool down these structures cracked. The glue used (Masterbond EP29LPSPA0-1 BLACK) has good thermal properties at low temperatures, but it was concluded that the thermal stress caused by the different expansions of Si and Zirconia caused the cracking of the Si wafer.

Good progress was made when switching to fibre components made of silica, as they have closer agreement in thermal expansion behaviour with Si. Diodes with a back side lens and a larger aperture of 100  $\mu\text{m}$  (model PDCS24L) made the alignment easier. An example of the stud bumps and aperture is shown in Figure 1.7. A novel structure (interposer) with laser cut holes was developed and flip chip glued over the diodes, so that fibre components could be manually inserted in the openings, for a self-aligned system. Examples

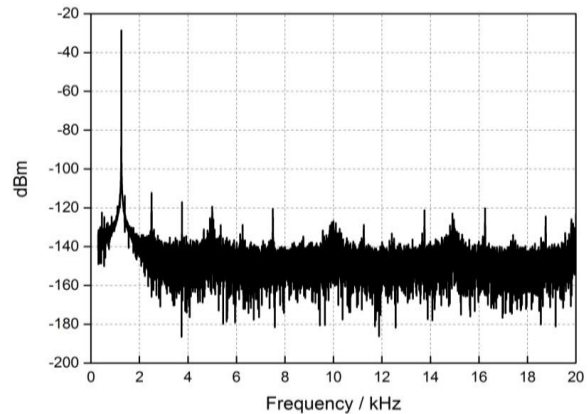


**Figure 1.6:** Frequency spectrum of a sinusoidal waveform with a frequency of 1.25 kHz and an RMS output voltage of 5.8 mV synthesized in the INRIM cryo-cooler system using a series array consisting of 4000 Josephson junctions. Higher harmonics are suppressed by more than 80 dBc.

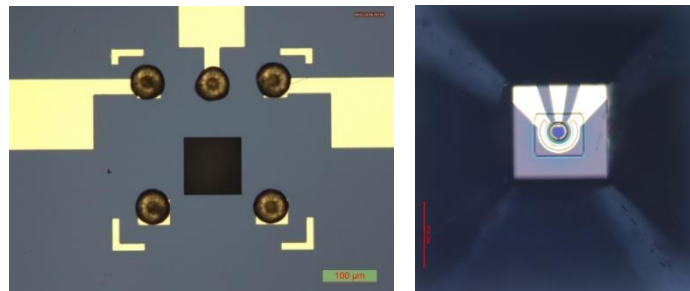


**Figure 1.7:** Photograph showing the structure of the stud bumps on the carrier, and a visual inspection of the aperture of the diode after flip chip bonding.

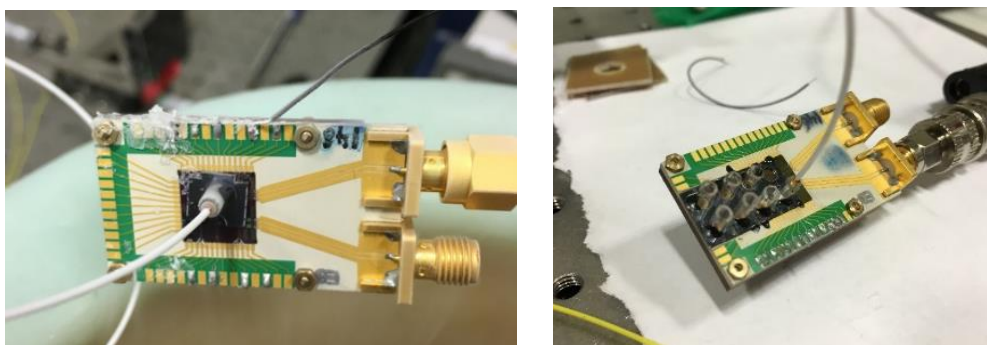


**Figure 1.8:** a) Successful testing of device with single diode at 77 K. b) Sample with 8 flip-chip bonded diodes with fibre alignment sleeves.

of single and eight fibre versions are shown in Figure 1.8.

These devices were stable during tests at both 77 K and 4 K. However, problems with loss of signal during cooling in liquid Helium, still remain to be solved. Tests in cryocoolers with vacuum chambers will be performed in order to eliminate the risk of forming nitrogen ice on the lens. The mechanical properties of the structure is stable during several cool downs to 4 K, and the diodes provide around 23 mA under stable illumination at 77 K (in liquid nitrogen).

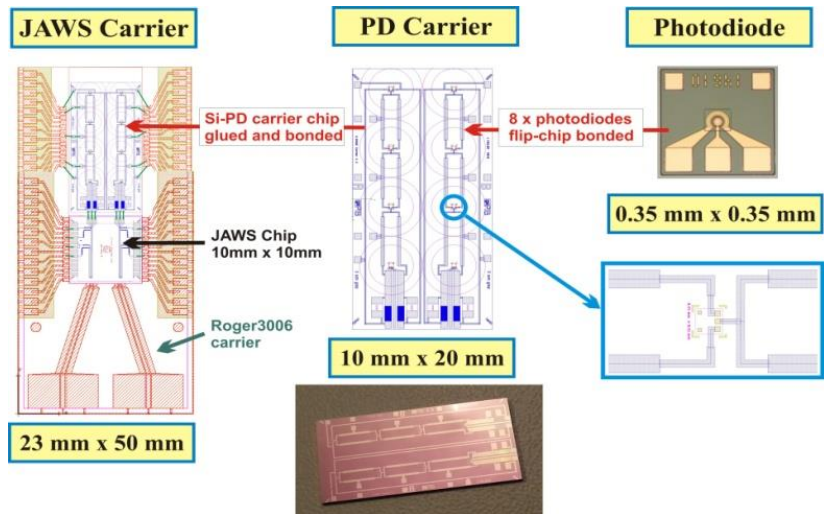


**Figure 1.9:** Concept of the carriers. Left: main carrier, middle: photodiode carrier (top: layout, bottom: photo), right: photo of a photodiode (top) and detail of the carrier for mounting the photodiode (bottom).

Suitable carriers have been developed for mounting and to transmit the short current pulses delivered by the photodiodes to the Josephson arrays (cf. Figure 1.9). The carriers were designed, fabricated, tested and improved. The main carriers were made from Rogers 3006. The photodiode carriers contain special alignment and bonding-pad structures and are optimized for flip-chip bonding of the lensed photodiodes. The high-frequency transmission lines were realised as coplanar waveguide transmission lines (CPW) fabricated on Silicon wafers.

### 3.1.3 Optoelectronic pulse generation system

An optoelectronic pulse generation system was developed at NPL using commercial equipment operating at the telecoms wavelength of 1550 nm (Figure 1.10). Two Mach Zehnder modulators (MZM) were used; the first to convert electrical pulses to optical pulses and the second to remove the complement code pulses in order to produce zero optical signal for the false code. To optimise the extinction of the pulses, the jitter in the system had to be minimised so that the clock controlling the second MZM was adequately synchronised to the master clock (from which the original code is generated). An example of the optical pulse code is shown in the bottom right of Figure 1.10, showing generation of TRUE and FALSE codes.

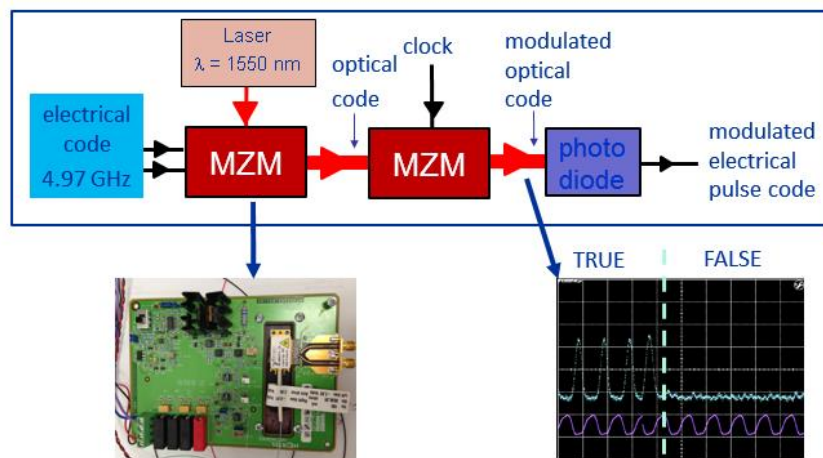


**Figure 1.10:** Diagram of optoelectronic pulse generation system. Electrical pulse code is sent to a Mach Zehnder modulator (MZM) which produces the corresponding optical code. Due to the AC coupling of the pulse drive electronics the complement of the code must be sent during the FALSE phase. These pulses are then removed using a second MZM, operating via a synchronised and phase shifted clock. An oscilloscope trace of the modified optical code is shown, demonstrating the extinction of the pulses during the FALSE phase. An erbium doped fibre amplifier and notch filter (not shown) were required to increase the optical pulse height before applying them to the photodiode to drive the array.

### 3.1.4 Delta Sigma electronics

A first order delta sigma modulator based on a low noise high bandwidth op-amp was designed, built and tested at NPL (Figure 1.11). This formed a combined difference amplifier and integrator. The input noise of the system was measured for various combinations of circuit components and shown to give a signal to noise ratio of the order of  $10^4$ . The bandwidth of the system was measured to be about 1 MHz.

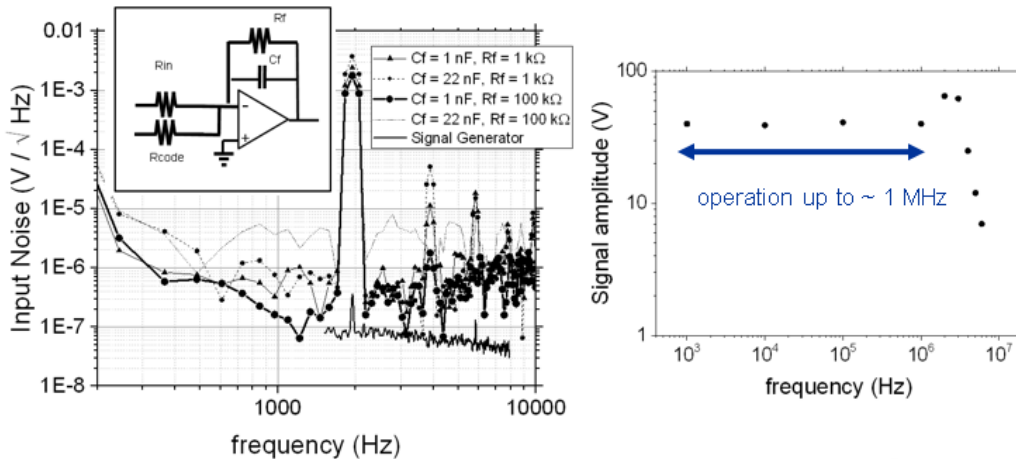


**Figure 1.11:** The input noise of the delta sigma electronics as a function of frequency (left). Inset shows the circuit diagram of the first order delta sigma modulator. The system was shown to operate up to a bandwidth of 1 MHz (right).

The above analogue delta sigma stages were then combined with the components shown in Figure 1.12 to produce the feedback loop. A particular challenge was to generate GHz rate pulses (which are required to drive the Josephson array) from a feedback loop operating at a much lower frequency (19.44 MHz). This was achieved using a FPGA (field programmable gate array) to read the output of the comparator and write either a TRUE or FALSE 16 bit code to the serialiser. The serialiser converts this parallel code to a series of 5 GHz pulses and repeats this until the next code is received. The FPGA is controlled via a master clock (which is generated by a Si Labs clock generator). A multiple of the master clock signal is used to synchronise the serialiser so that the output code is locked to the feedback loop rate. The FPGA was programmed using National Instruments software and the read-write delay was reduced to around 10 ns.

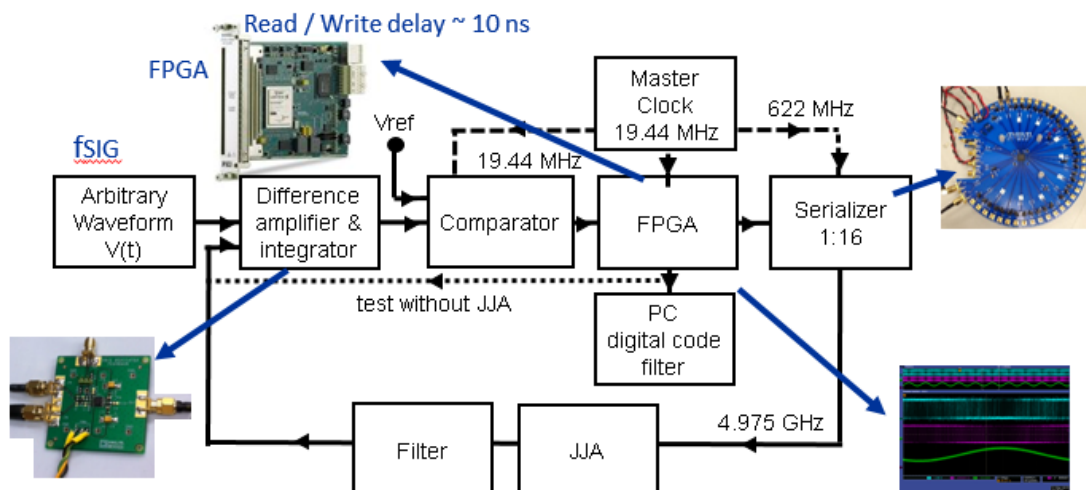


**Figure 1.12:** Schematic of delta sigma electronics. The feedback loop is controlled by a master clock operating at 19.44 MHz. Data from the comparator is read on each tick of the master clock by the FPGA. A code is then sent to the serialiser which produces GHz rate pulses which repeat until the next reading is made. The system can be tested without the Josephson junction array (JJA) by sending the pulse code directly back into the delta sigma electronics (dotted line). The optoelectronic components described above (not shown) are required to convert the serialiser pulses into optical pulses for optical drive.

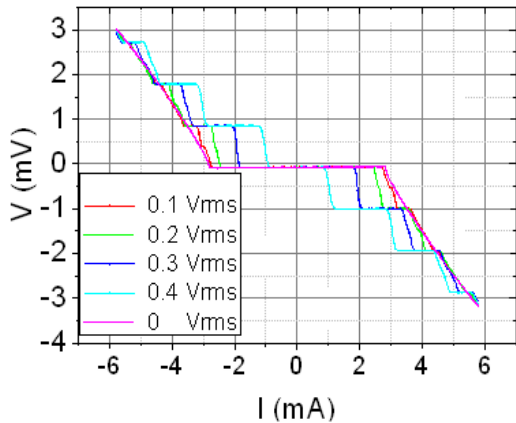


**Figure 1.13:** Current voltage characteristic of a 100 junction array when a 6 GHz sine wave is applied showing the variation of the constant-voltage steps as a function of sine wave amplitude.

The system components for the Josephson ADC have been characterised separately as well as in the following combinations: electrical drive of array (Figure 1.13), optical drive of array (Figure 1.14), delta sigma feedback loop with direct feedback (Figure 1.11) and delta sigma feedback loop with room temperature photodiode feedback.

An alternative system (Figure 1.15) was also developed in parallel, where a 250 MS/s 16 bit ADC is used as a quantizer which directly samples the integrator output making this a multilevel DS modulator, thus lowering the quantization noise in the band of interest. In addition, the high sampling rate of the ADC enables a higher oversampling ratio. The internal serializer-deserializer (SERDES) of the FPGA

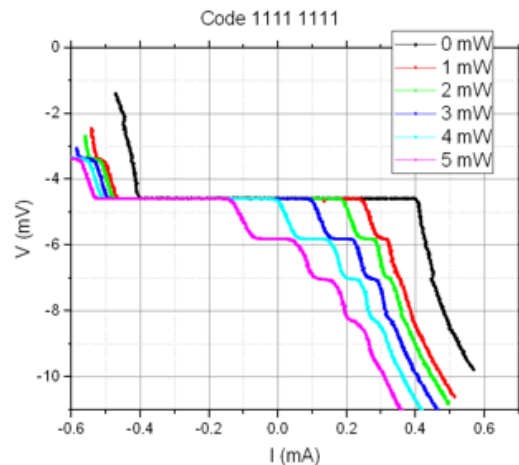
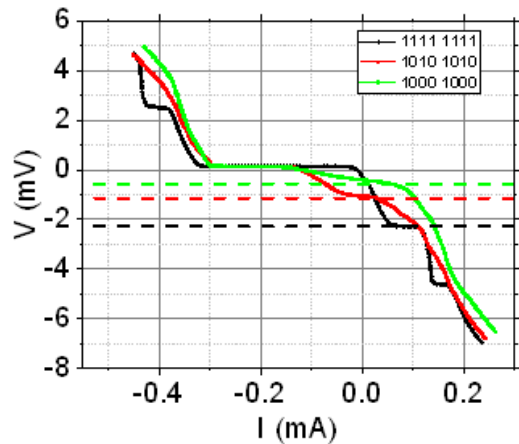


**Figure 1.14:** Generation of quantised voltage using optical pulse code. The voltage scales in proportion to the pattern sent to the array (top). The voltage steps vary with increasing optical power (bottom).

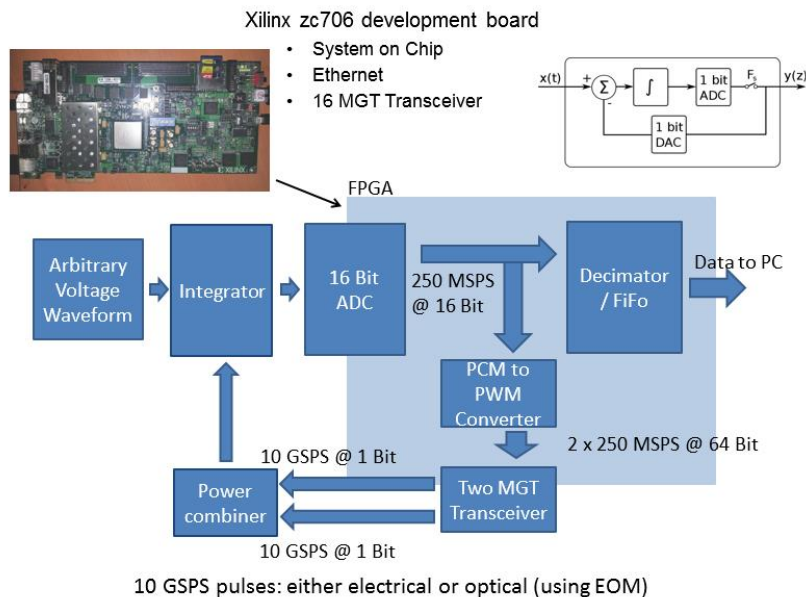


**Figure 1.15:** Schematic of alternative multilevel delta sigma electronics developed at VSL.



is utilized to produce fast pulses either electrically or optically. The latter is achieved by using commercial optical SFP+ modules which have bit rates > 10 Gb/s. Two optical streams containing the serialized code can be generated, one for the positive and other for the negative pulses to be sent to the Josephson array.

### 3.1.5 Conclusion

In this project a new measurement system for dynamic calibration of analogue-to-digital and digital-to-analogue converters has been designed and built. Key achievements beyond existing technology were the development of:

- Improved series arrays of Josephson junctions;
- 1 V RMS output voltages using pulse-driven arrays;
- A technique for mounting photodiodes for operation at low temperature;
- Delta sigma electronics for quantum voltage application;
- New method of producing optical pulse stream.

In conclusion, the components of a system for dynamic calibration of ADCs and DACs, based on the Josephson effect have been developed. Various Josephson arrays have been successfully operated as quantum voltage standards for dissemination methods (cf. section 3.2). A major breakthrough was the synthesis of waveforms with an RMS output voltage of 1 V. A technique for mounting high bandwidth photodiodes at low temperature to enable optical drive of the Josephson array has been developed. Delta sigma electronics have been built and demonstrated in a variety of feedback loop configurations including the use of the new optoelectronic pulse generation system. In this way proof of concept for an optical pulse driven Josephson array based quantum voltage digitiser has been demonstrated. Although time did not allow completion of evaluation of the photodiode at low temperature in the delta sigma loop, the alternative measurements undertaken with a room temperature photodiode are adequate to achieve the scope of the objective. The results and information obtained in this project will be vital in future work to develop this system further towards a commercial measurement capability.

## 3.2 Dissemination methods

Work on this objective was important to bridge the gap between quantum-based waveform standards and the test and calibration needs from semiconductor industry and instrumentation manufacturers for analogue-to-digital (ADC) and digital-to-analogue (DAC) converters. The link was established by the development of dissemination methods focused on the frequency range from DC to the MHz range and voltages up to 10 V and based on state of the art instrumentation and converters including techniques for both repetitive and single shot waveforms. Advantage has been taken of already existing, worldwide unique equipment to make a step change from thermal transfer based calibrations to sampling measurements.

The first part of this work was focused on how to characterise high-precision sampling equipment using optimised quantum-based systems (section 3.2.1). As a second activity, DAC-based sources have been developed and exploited to meet specific requirements for sampling in industry (section 3.2.2). The third part was to validate the step change from thermal transfer based calibrations to sampling measurements (section 3.2.3).

### 3.2.1 Quantum-based characterisation of ADC

The aim of this part of the project was to use quantum-based reference equipment to test present state-of-the-art ultrahigh performance commercial sampling equipment. For this, some equipment and/or measurement procedures have been investigated in detail and improved. Different approaches are presented and described in this section.

#### 3.2.1.1 Josephson mercury wetted relay step generator

An ideal voltage step, i.e. an infinitely fast non-oscillating transition from one DC voltage to another, is a multi-tone source extending from very low to very high frequencies. Sampling a nearly-ideal step voltage source and comparing the recorded set of samples to an ideal set can therefore in principle give the

information of the whole frequency response of a precision sampler at a single sweep. Using a Josephson voltage standard to set the amplitude of the step voltage could be a complementary approach for characterising sampling devices.

A close-to-ideal step excitation source is a mercury-wetted relay. This switch device is exceptional in a sense that the closing time is fast ( $< 1$  ns) and the contact formation is completely bounceless, i.e. free of oscillations. VTT studied the ultimate uncertainty limits of this technique in low voltage sampler investigations. Figure 2.1a depicts the structure of the relay. A stable DC voltage is connected to the “dc in” connector, the device under test to the “Step out” connector and a synthesizer for triggering the relay to the “trigger in” connector. The trigger signal results in closing the relay, and a short circuit is formed to the input of the device under test so that the voltage step is delivered to the device under test.

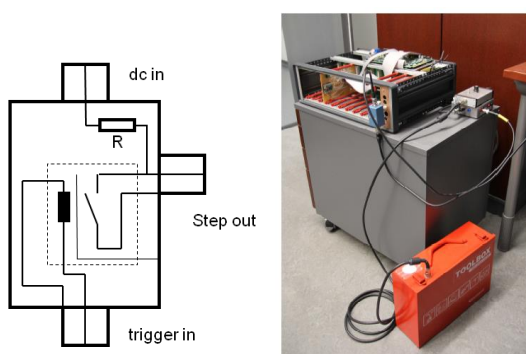


**Figure 2.1:** a) Internal connection of the step generator box and b) test setup.

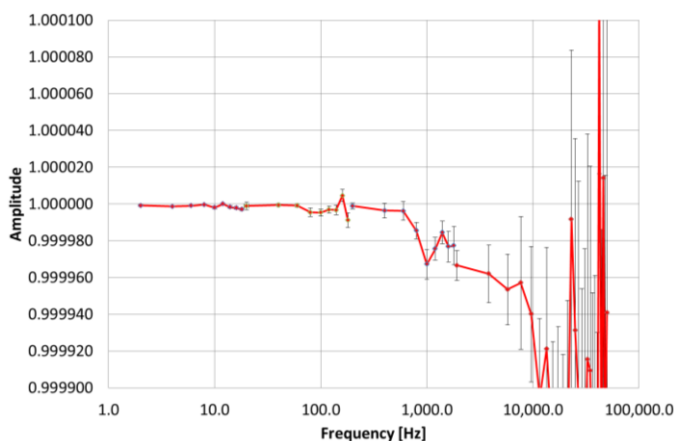


**Figure 2.2:** The estimated frequency response of VTT's 18 bit digitizer. The response is calculated from 300 steps sampled at 100 kS/s. Each record contained ca. 50000 sampled points, i.e. record length was 0.5 s. Error bars show one standard deviation of the mean.

Three step voltage generators have been built and different filtering schemes tested. In addition, the sampling strategy and signal processing schemes were investigated. It turned out that at the current status, the Josephson voltage standard could be replaced with a Zener voltage standard as a DC reference without any loss of performance of the system since the noise of the sampler was dominating. The test setup is shown in Figure 2.1b. The step generator box (blue) is connected directly to the input of the digitizer. The DC voltage to the generator is fed from a Zener reference (grey box on the right side of the digitizer) powered by a battery (red, on the floor). The generator is triggered by a commercial function generator (not in the picture). The digitizer sample rate was set to 100 kS/s, and 300 records of 49,980 samples were collected. The records were triggered on the falling edge of the signal. The record length was approximately 0.5 seconds. Step repetition rate was about 0.2 Hz. Figure 2.2 shows an example of results obtained from measurements performed with a 18-bit digitizer made at VTT. 300 sampled steps were averaged to obtain the frequency response. Further work is needed to validate the results with a quantum ac voltage standard.

### 3.2.1.2 Delta-sigma PJVS

SP constructed a waveform source based on a programmable Josephson voltage standard (PJVS). This source aimed to serve as a reference for calibrating high performance digitizers. To overcome the limitations in resolution and sampling rate, allowing only stepwise approximated waveforms, Delta-Sigma modulation (Figure 2.3) was used together with specially constructed low pass filters (Figure 2.4). Waveforms were generated with very high spectral purity (Figure 2.5), allowing to detect non-linearities in a digitizer at a very low level, better than 120 dB below the fundamental (Figure 2.6). However, the amplitude accuracy required for precision measurements could not be verified.

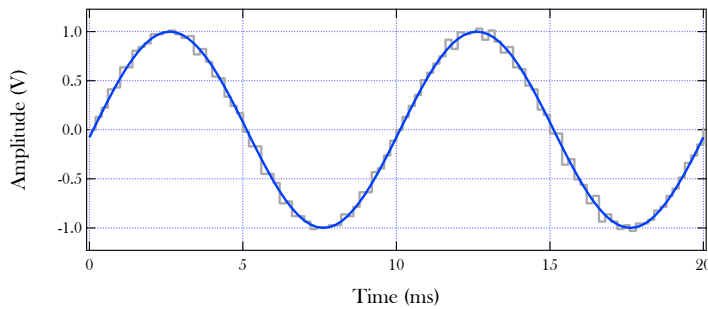


**Figure 2.3:** A Delta-Sigma modulated signal (grey) looks very noisy at first glance, but the noise is concentrated at high frequency, and can be efficiently removed with a low pass filter. The resulting signal (blue) is a smooth spectrally pure waveform.

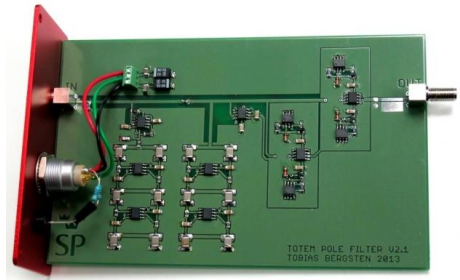


**Figure 2.4:** Custom low pass filter. This filter constructed for this application is very stable and has low distortion, allowing a very accurate and spectrally pure waveform to be generated.

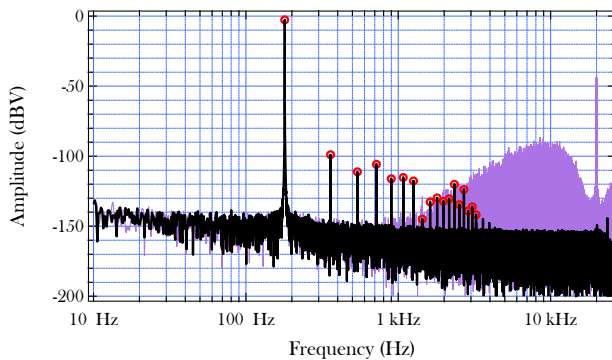


**Figure 2.5:** Frequency spectrum of a 180 Hz signal generated by a programmable Josephson voltage standard (PJVS). The signal from the PJVS was Delta-Sigma modulated and filtered with a 210 Hz 5<sup>th</sup> order low pass Butterworth filter. The harmonics are caused by distortion in the digitizer. The purple spectrum is the unfiltered signal.

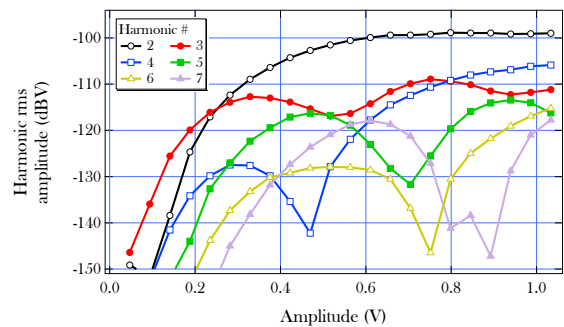


**Figure 2.6:** The harmonic amplitudes of the sampled signal as a function of the fundamental amplitude can serve as a representation of the non-linearity of the digitizer.

### 3.2.1.3 PJVS test bench

A Josephson-based test bench operated at METAS was used for the characterisation of the ADC both in the time and frequency domains.<sup>5</sup> The schematic of the test bench is shown in Figure 2.7. The Programmable Josephson voltage standard (PJVS) supplies the reference voltage waveforms directly to the digitizer under test (DUT). The design and operation of the PJVS is based on a commercial SNS Josephson junction array. The maximum voltage provided by the Josephson junction array at 70 GHz is 1.18 V. Both the PJVS and the DUT are frequency locked to the same reference signal of 10 MHz provided by a Cs clock. Moreover, the Josephson bias current source supplies the trigger signal to synchronize the digitizer to the Josephson stepwise waveform. Both the clock and the trigger signals are optically distributed to avoid spurious coupling between the various components of the system. The first computer is dedicated to fully control the

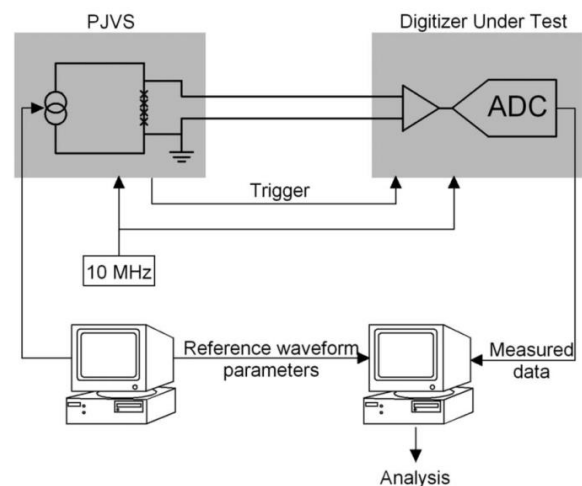


**Figure 2.7:** Schematic of the METAS test bench using the PJVS to generate the reference signal measured by the DUT.

<sup>5</sup> F. Overney, A. Rüfenacht, J.-P. Braun, B. Jeanneret, P.S. Wright, *Characterisation of metrological grade analog-to-digital converters*, IEEE Trans. Instrum. Meas. **60** (2011), 2172 – 2177.

reference voltage generated by the PJVS. Reference waveform parameters are sent to the second computer, which also gathers the measured data from the digitizer for further analysis.

### The equivalent time sampling method

The frequency range in which the DUT can be characterised is limited by its sampling frequency. The goal is to extend the frequency range over which the ADC can be calibrated with the PJVS. For this purpose, an oversampling method can be applied which is called Equivalent Time Sampling (ETS), see Figure 2.8. This method is described in detail in published papers <sup>6, 7, [3]</sup> and in the good practice guide delivered within the project [G1].

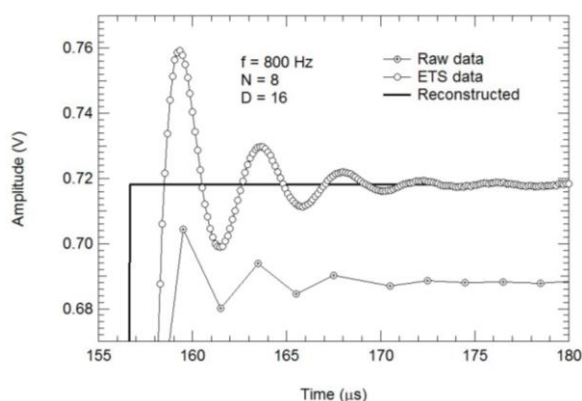


**Figure 2.8:** The raw data curve is the amplitude of one Josephson step measured with the digitizer at a sampling frequency of  $f_s = 468.75$  kHz. This curve was shifted by  $-0.03$  V for clarity. The oversampling procedure resulted in the curve ETS data showing a more detailed information corresponding to an equivalent sampling frequency of  $f_{eq} = 7.5$  MHz.

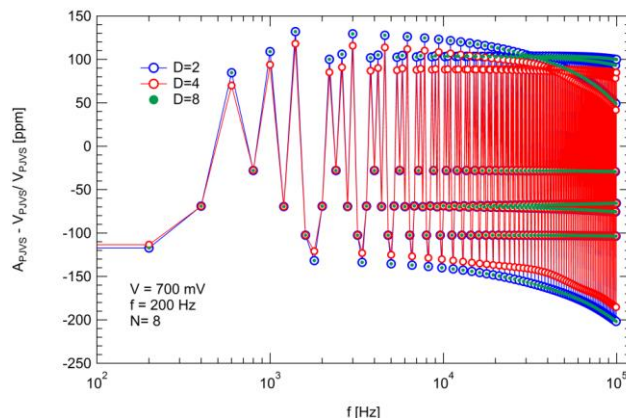


**Figure 2.9:** Relative difference between the sampled waveform and the theoretical waveform calculated on the basis of  $K_{J-90}$  (see [3] for details). The fundamental frequency is 200 Hz and the RMS amplitude 0.7 V. Three measurements were performed at various multiplier,  $D = 2, 4, 8$  leading to the same equivalent frequency of  $f_{eq} = 1.875$  MHz for the three curves.

The measured PJVS spectrum can be compared with the one obtained from the theoretical voltage  $V_{PJVS}$  which is determined with a DFT on the ideal stepwise waveform where each voltage step is calculated with the Josephson constant  $K_{J-90}$ . The result of this comparison is plotted in Figure 2.9 up to a frequency of 100 kHz.

#### 3.2.1.4 Pulse-driven Josephson arrays

As pulse-driven Josephson arrays enable quantum-accurate waveforms to be synthesised, they were of special interest for this project. The low RMS output voltage of 250 mV at most at the beginning of the project limited the application of pulse-driven systems significantly. The breakthrough with the development of a 1 V system (section 3.1.1.2) significantly extends the possible application areas. A direct comparison of the 1 V pulse-driven system and the AC Quantum Voltmeter was performed at PTB, in order to check the system. The comparison demonstrated an excellent agreement between the two quantum standards with  $(3.5 \pm 11.7) \cdot 10^{-9}$  in relative units ( $k = 1$ ). A paper was published in the journal *Metrologia* and was selected as one of the highlight papers in 2015 [4].

Pulse-driven Josephson arrays have been used for further investigations, especially at higher frequencies up to the MHz range and for measurements that require pure frequency spectra (cf. examples below).

#### Pulse-driven Josephson arrays operated in a small cryostat

The voltage leads and connection cables of the pulse-driven arrays for AC Josephson voltage standards (ACJVS) cause the output voltage to show deviations that scale with frequency squared. In this work, deviations of almost 1 % at 1 MHz have been reported for a cryostat with voltage leads of about 1.5 m.<sup>8</sup> For

<sup>6</sup> IEEE Standard for Terminology and Test Methods for Analog-to-Digital Converters, IEEE Std. 1241 2000, 2000.

<sup>7</sup> IEEE Standard for Digitizing Waveform Recorders, IEEE Std. 1057-2007, 2007.

<sup>8</sup> H.E. van den Brom and E. Houtzager, *Voltage lead corrections for a pulse-driven ac Josephson voltage standard*, *Meas. Sci. Technol.* **23** (2012) 124007 (7 pp.).

practical applications, this limits the ACJVS output frequency to approximately 100 kHz. The initial goal of this project was to increase this upper frequency to 10 MHz. However, recently we found that the frequency dependence is caused by reflection of waves at the high impedance of the load [5]. Based on these findings the characterisation of ADCs in time and frequency domains using arbitrary waveforms was focused on frequencies below 100 kHz.

VSL and PTB performed measurements obtained using a He-4 cryostat at PTB with a short cryoprobe with voltage leads of about 70 cm only [6]. This is to suppress the effect of the voltage leads causing the output voltage to deviate significantly from the voltage on the chip. In the pulse-driven ACJVS at PTB, a chip with two arrays of 9,000 junctions each was installed for the measurements described here. The ACJVS output voltage was connected directly to a commercial AC-DC thermal transfer standard (TTS) under investigation (Figure 2.10).

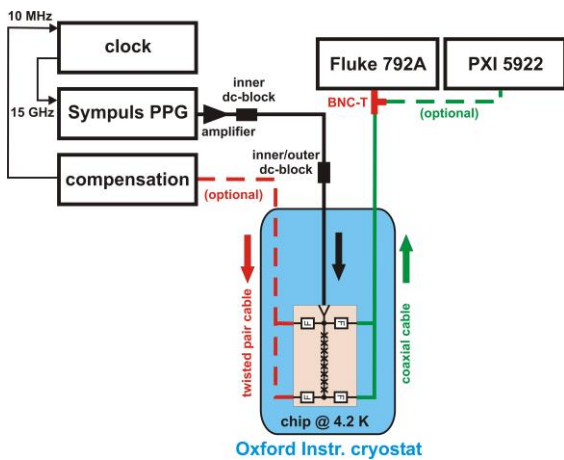


**Figure 2.10:** Simplified measurement setup of the small cryostat.

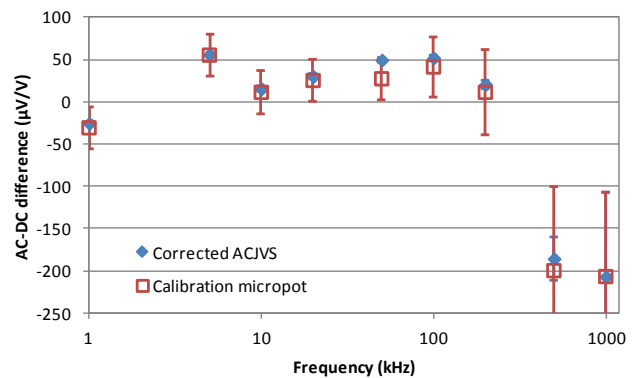


**Figure 2.11:** ACJVS results for the AC-DC difference of the TTS at 20 mV as compared to the PTB micropot calibration results. Note that the compensation method defines 1 MHz values to be identical.

The deviation at higher frequency was an order of magnitude smaller than was observed before with a normal cryostat, i.e., only 750  $\mu\text{V/V}$  at 1 MHz instead of almost 10 mV/V. The observed square dependence on the signal frequency and cable length follows exactly the expected behaviour. The measurements at lower frequencies were corrected based on the PTB micropot calibration result at 1 MHz, assuming squared frequency dependence.<sup>8</sup> Figure 2.11 shows that the ACJVS results found this way agree well with the micropot results. Note that by definition of our compensation method the micropot results and the corrected ACJVS results at 1 MHz agree.

Furthermore, the influence of connecting other cables and equipment was investigated. For the largest cable of 127 cm we found a deviation of 0.34 % at 1 MHz; when assuming the path length within the cryoprobe and within the TTS to be 89.5 cm the deviation showed a square dependence on cable length as predicted [6]. The results support the explanation of the frequency dependence in terms of standing waves.

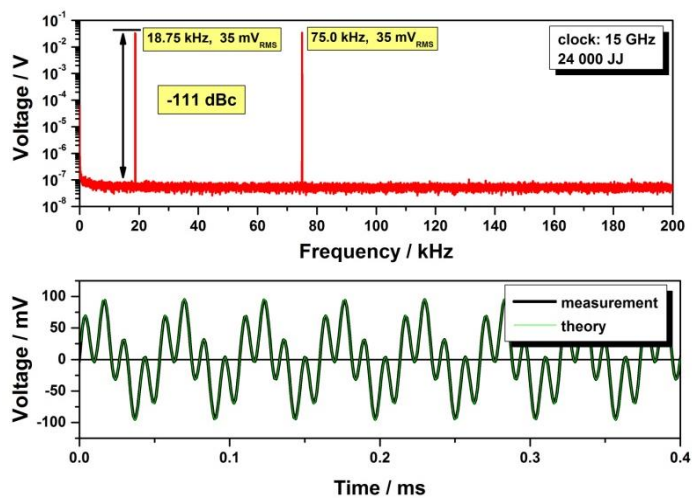


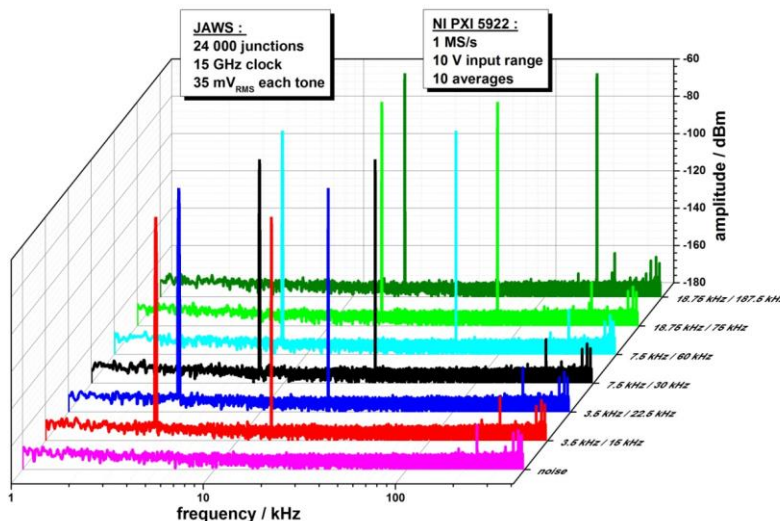
**Figure 2.12:** Measurements of a two-tone signal generated with a pulse-driven ACJVS as performed using an NI 5922 PXI DAC. The upper plot shows the data in the frequency domain and the lower plot shows the time domain.

Pulse-driven Josephson arrays for synthesis of arbitrary waveforms

The pulse-driven ACJVS at PTB was used to generate different two-tone signals with 35 mV RMS per tone. Figure 2.12 shows measurements as performed by the NI 5922 PXI in the frequency domain (spectrum) and the time domain for a signal with tones at 18.75 kHz and 75 kHz. The data in the time domain demonstrate that the theoretical curve and the measurements coincide within the noise. The spectrum confirms that no second-order effects are visible above the noise floor, which is -111 dB below the two tones in this case.

Figure 2.13 shows the measured spectra (amplitude as a function of frequency) for the different signals. No signals with sum or difference frequencies were measured above the noise floor, which is better than 111 dBc for all curves.

These measurement results show that the linearity of the device under test is on the order of  $10^{-6}$ , over the whole frequency range up to 200 kHz. This number can be improved by an order of magnitude by increasing the output voltage to 1 V, leading to testing linearity up to the  $10^{-7}$  level or better. Note that this number is limited by the noise floor of the digitizer.



PTB, Kieler, 2016

**Figure 2.13:** Spectra of different two-tone signal generated with a pulse-driven ACJVS as performed using an NI 5922 PXI DAC. The light-green curve (18.75 kHz / 75 kHz) represents the same data as shown in Figure 2.12.

**3.2.2 Development and use of DAC-based AC voltage reference sources**

Two DAC-based AC voltage reference sources have been developed, improved and investigated in this project. These activities are described in this section.

**3.2.2.1 High-stability arbitrary waveform generator DualDAC**

A highly stable arbitrary waveform generator based on electronic DACs has been designed and built at VTT. For the first time, a voltage source specifically designed to disseminate the SI volt in terms of waveforms other than only pure sine waves has been built. The source, now also commercially available as DualDAC2 from Aivon Ltd (Helsinki, Finland), is shown in Figure 2.14. Within the project, this new instrument has been shown to have a potential to be used even as a travelling standard between NMIs possessing AC quantum standards and the next tier of users like calibration laboratories or instrument manufacturers.



**Figure 2.14:** DualDAC2, a new arbitrary waveform generator for disseminating SI volt in terms of arbitrary voltage waveforms.



Until now, primary tools for calibrating precision instruments in AC voltages outside NMIs have been electronic sources called calibrators which provide a large range of different AC voltage and current signals. However, only purely sinusoidal waveforms are available from these and their synchronization properties are not ideal for sampling measurements. Arbitrary waveform generators which have been commercially available are not sufficiently stable for calibration purposes, with the uncertainty of AC voltage (RMS) being typically in the range of tens of  $10^{-6}$  rather than in the required  $10^{-6}$  range. In a nutshell, no dissemination tools of SI traceable arbitrary voltage waveforms with sufficiently low uncertainty have been available.

To improve this situation VTT started building up on previous work in iMERA-plus project JoSy to design and realize a new synthesizer. Quintessential for the success of the work was collaboration with PTB that has recently developed an AC quantum voltmeter (AC QVM) which allows measuring (sampling) the produced waveform in terms of SI volt. With the help of this unique system the output waveform properties could be measured with accuracy below 1 part in  $10^6$  and problems in the synthesizer design solved.

Figure 2.15 shows an example of a multi-tone waveform produced with DualDAC2 (black trace), the corresponding AC QVM waveform (red) used in the measurement and the difference between these two signals in blue. The RMS voltage of the produced waveform could be measured with a relative accuracy of 5 parts in  $10^8$  in 200 seconds. Harmonic analysis of the spectral components of the waveform is also feasible with an uncertainty of  $10^{-6}$  in less than one second data acquisition time.

To investigate the feasibility of using the new source as a travelling standard, five project partners (VTT, PTB, CMI, CEM, TUBITAK) took part in a circulation where six different waveforms had been chosen to be investigated with various measurement techniques. The waveforms were measured with the PTB AC QVM at the beginning and end of the loop for best possible monitoring of the stability of the source over the half-a-year long period. The results of the comparison demonstrate that the source is

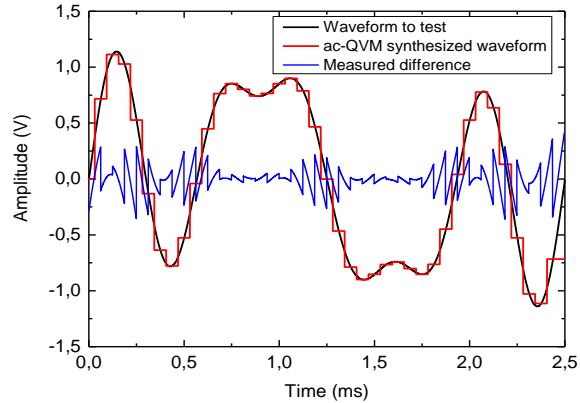


Figure 2.15: A multi-tone voltage waveform produced with DualDAC2 and measured with AC quantum voltmeter of PTB.

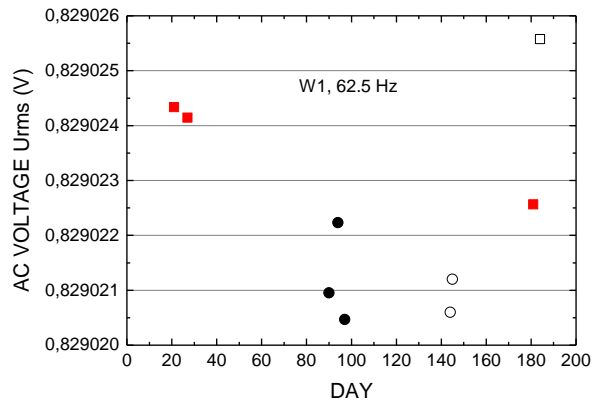


Figure 2.16: Example of results of five NMIs participating in a circulation of DualDAC2. Measurement results of AC voltage (RMS) of a 62.5 Hz 1.18 V pure sinusoidal signal are shown. Possible corrections based on simple DC voltage measurements performed by the partners probably decrease the scatter of the data (preliminary claim). Even without the corrections the results demonstrate that the source is sufficiently stable to bring new value to disseminating SI volt to characterisation of precision instrumentation.

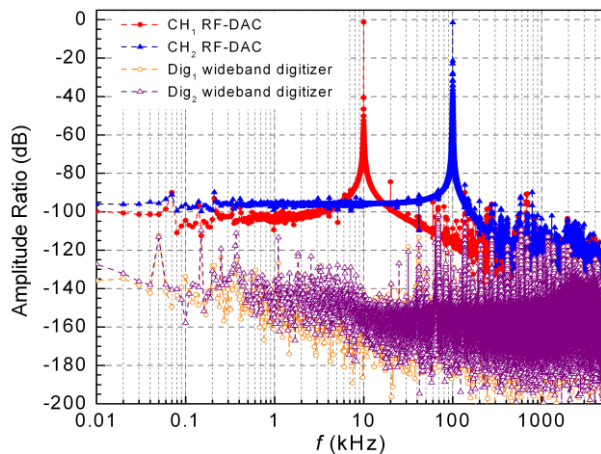


Figure 2.17: Frequency spectrum of 10 kHz and 100 kHz sine waves synthesized simultaneously by the dual output HS-DAC based semiconductor and the noise floor of the sampling system based on wideband high-precision digitisers.

sufficiently robust and stable to be used as a dissemination tool of arbitrary voltage waveforms for calibration of precision sampling instruments and AD converters. Figure 2.16 gives an example of results obtained by the five participating NMI's measuring a pure sinusoidal wave at 62.5 Hz frequency and 1.18 V amplitude. All the data are within  $\pm 3 \cdot 10^{-6}$  envelope, and taking into account special monitoring point voltages, the scatter would evidently decrease at least by a factor of two (preliminary results).

### 3.2.2.2 Wideband DAC-based synthesiser

INRIM has developed, tested and improved a DAC-based synthesiser (dual-channel 1 GSample/s, 16 bit, THD < -96 dB at 100 kHz) to be used as a transfer standard for the calibration of high precision digitizers beyond the acoustic band (Figure 2.17). The voltage output of the synthesiser has been increased up to 7 V for frequencies up to 1 MHz. High-precision measurements were performed at PTB with pulse-driven Josephson arrays (cf. Figure 2.18). Different waveforms with high spectral purity and amplitudes of about 100 mV were directly transferred to the high-speed DAC synthesiser by using a synchronous detection principle based on a lock-in detector. Figure 2.19 shows the DAC-based synthesiser in use.

The comparison between the high speed semiconductor and superconductor sources was performed for frequencies ranging from 10 kHz to 100 kHz by using a compensated resistive voltage divider with nominal ration of 1:10. The detection principle employed imposes stringent constraints in relation to the frequency locking between the sources as well as timing required for optimization of all measurement parameters. In particular, the in-phase and quadrature components of the residual voltage difference detected by a phase sensitive detector were within several microvolts, e.g. at 100 kHz both components were lower than 1  $\mu$ V and the short time stability was measured to be better than 500 nV within a few minutes.



**Figure 2.18:** Experimental setup at PTB for the direct transfer of high purity quantum waves to the high-speed DAC-based synthesiser. A synchronous detection approach was employed for the characterisation of the HS-DAC in terms of high purity quantum waves synthesized by a pulse-driven Josephson array operating in a cryo-cooler setup (PTB).



**Figure 2.19:** Example of use of the HS-DAC for the characterisation of high precision wideband digitizers.

### 3.2.3 Comparison and validation of sampling methods

Extensive measurements and comparisons have been performed, in order to validate the different systems including the sampling measurement techniques. For these investigations, different quantum based systems have been used as programmable Josephson voltage standards as well as the AC Quantum Voltmeter, pulse-driven Josephson voltage standards, and the combined system containing a pulse-driven and a programmable Josephson Voltage Standard. These systems have been applied for detailed investigations of thermal transfer standard measurements and the DualDAC2. In addition, an inter-comparison was performed to confirm properties and stability of the DualDAC 2 using thermal transfer standards.

### 3.2.3.1 Comparing sampling and thermal techniques

PTB has used the pulse-driven Josephson voltage standard (JVS) to suppress the unwanted higher harmonics generated by the Programmable Josephson Voltage Standard (PJVS) to generate quantum-based arbitrary waveforms at 1 V. The set-up of this combined Josephson system<sup>9</sup> is shown in Figure 2.20. The yellow box indicates the ADC (NI PXI 5922) which has been used to measure the spectrum and the waveforms. The waveforms (time domain) were used as basis for further iteration of the delta-sigma code. The spectrum for a sine wave of the combined system without iteration process has been compared with the spectrum after the first iteration process. An improvement from 0<sup>th</sup> to 1<sup>st</sup> iteration was observed. Higher harmonic tones have been suppressed from about -110 dBc to -126 dBc, which is the limit of the ADC.

Intensive investigations have been performed for sine waves. The transconductance amplifier from NMIA has been used to measure the combined system with a thermal converter at the 1 V level within the frequency range from about 150 Hz to 1 kHz. The same signals (time domain and frequency spectrum up to 500 kHz) have been measured at PTB with the AC quantum voltmeter. The measurements using both methods agree well. Slopes on a trim current variation on the PJVS (transients) have been improved by an iteration process for the pulse-driven JVS. However, the slopes could not be completely compensated (limited bandwidth of the PXI), thus uncertainties were limited to a few parts in 10<sup>6</sup>.

Arbitrary waveforms with higher harmonic tones have also been investigated. A frequency spectrum is shown in Figure 2.21. The higher harmonic tone is synthesized only by the pulse-driven JVS. As for sine waves, arbitrary waveforms (e.g. a 1 V sine wave at 156.25 Hz with additional 1 mV 12<sup>th</sup> harmonic tone (1875 Hz)) could not be significantly improved by an iteration process for the pulse-driven JVS because the slopes cannot be completely compensated. An additional 1 mV tone only affects the RMS value for the thermal transfer standard (TTS) by 1  $\mu$ V/V which is of the order of variations due to slope changes. Therefore, this additional peak is almost invisible. For all TTS measurements the uncertainties were limited to a few parts in 10<sup>6</sup>.

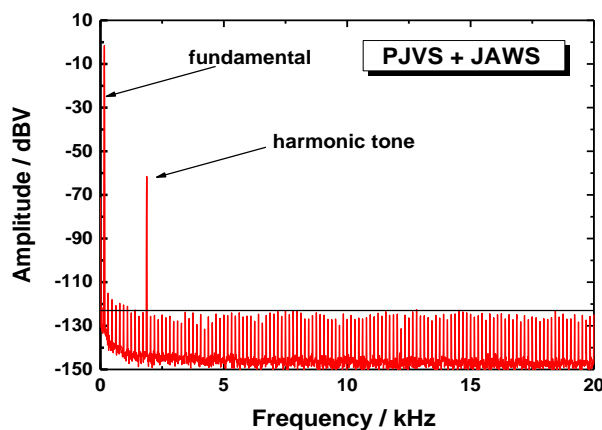


Figure 2.21: Frequency spectrum for the combined system of PJVS and pulse-driven JVS including a higher harmonic tone.

### 3.2.3.2 Inter-comparison

To confirm properties and stability of the generator DualDAC2 (section 3.2.2.1), an inter-comparison was planned and performed. The second aim here was to try out an inter-comparison based on multi-tone signals. The device circulated between several laboratories and was measured and evaluated by means of thermal transfer standards and digital sampling techniques.

The DualDAC2 is able to generate customary waveforms; therefore several waveforms were prepared and used as a signal to be measured. The first waveform was a single tone signal, which was possible to measure either by thermal transfer standards or by sampling methods. The second waveform consisted of a sine wave with very small harmonic content still possible to measure by thermal transfer standards, however with inherent errors. The third waveform consisted of five harmonics, thus possible to measure accurately only by means of digital sampling and signal processing. PTB was selected as the reference laboratory and provided calibration of the DualDAC2 by means of ACJVS for all selected waveforms. The device circulated between the laboratories in the following order: PTB, CMI, CEM, TUBITAK and again PTB.

The results of the comparison showed that the measurement by means of thermal transfer standards is common and mastered. However, measurement by means of sampling leads to issues and the subsequent data processing required for multitone signals is still a novelty for metrological institutes. The voltage of the inner reference of the DualDAC2 changed only by  $3 \cdot 10^{-6}$  thus the device is very suitable as a reference standard. More details are presented in section 3.2.2.1.

<sup>9</sup> R. Behr, O.F. Kieler, D. Schleussner, L. Palafox, F. J. Ahlers, *Combining Josephson systems for spectrally pure AC waveforms with large amplitudes*, IEEE Trans. Instrum. Meas. **62** (2013) 1634-1639.



### 3.2.4 Conclusion

In this project we established new dissemination methods based on state of the art instrumentation and converters, including techniques for both repetitive and single shot waveforms. The key achievements beyond existing methods were:

- The development of improved Josephson mercury wetted relay step generator;
- Use of Programmable Josephson Voltage Standard (PJVS) test bench;
- Application of pulse-driven Josephson series arrays;
- Development and use of DAC-based AC voltage reference sources;
- Comparison and validation of sampling methods.

In conclusion, step voltage generators were built, used for initial investigations, and improved. Detailed investigations demonstrated the potential of the Programmable Josephson Voltage Standard test bench. Pulse-driven Josephson arrays operated in a small cryostat showed that the output voltage deviations above about 100 kHz are significantly reduced by short output cabling. Two highly stable arbitrary waveform generators based on electronic DACs have been designed, built and improved. An inter-comparison based on multi-tone signals was successfully performed using the DualDAC2.

## 3.3 Digital signal processing techniques

Digital signal processing techniques form a cornerstone of measurement systems based on sampled signal data. They can be used either to investigate phenomena in today's complex instrumentation or to estimate signal parameters retrieved from sampled series. While coherently (synchronously with an integer number of signal periods) sampled harmonic signals can be analysed straightforwardly using FFT with no additional errors, this is not the case when synchronisation is not possible. Therefore, special attention should be paid to errors possibly generated under non-coherently sampled conditions.

The aim of this work was to improve digital signal processing techniques and evaluate their contribution to the measurement uncertainty. A large number of digital signal processing techniques have therefore been studied. More than ten different digital signal estimation algorithms have been investigated and new techniques were developed. Further, traceability and measurement uncertainty concepts in digital sampling measurements were proposed to standard committee for inclusion in future standards in the related fields.

The first part of this work is focused on improved digital signal processing techniques for sampling measurements (section 3.3.1). As a second activity, contributions of signal processing on measurement uncertainties have been investigated and estimated including the development of a unique software toolbox (section 3.3.2). The third part was to identify metrology grade ADC parameters that require improved characterisation techniques from those already described by available standards (section 3.3.3).

### 3.3.1 Improved digital signal processing techniques

While signal sampling becomes a method of choice in the modern measurement systems, it also requires robust and accurate signal parameter estimation techniques. While this field already gained much attention in scientific and engineering community, the progress in this field has not matured yet. Some enhancements of investigations by SIQ and VSL to the state-of-the-art are given below.

#### 3.3.1.1 Improved sampled signal estimation for harmonically distorted signals

Single tone estimation algorithms provide simple, robust, fast and effective means to estimate sampled sine wave parameters. However, they are to a higher or lesser extent sensitive to harmonic distortions present in the signal. The improved procedure developed within the project works on already developed algorithms without introducing any modifications to them. By introducing quasi-coherent windowing, harmonic influence on the estimation of the fundamental signal parameters (including frequency) is reduced for most of the algorithms by orders of magnitude. Also, the noise performance of the algorithm used is not degraded, even if it has the disadvantage of having a slightly longer processing time.



Figure 3.1 shows an example of the enhanced performance for three algorithms (PSFE, IDFT2p and IDFT3p). A signal with 1 % second harmonic and 120 dB SNR was generated numerically and estimated for fundamental tone phase using the three algorithms while covering 6 to 7 fundamental periods. All three algorithms exhibit reduced error when sampling is close to coherent. This fact is actually used in splitting the sampled signal into two overlapping data windows of equal length, each covering (as close as possible) four periods of sampled signal. Signal estimation is performed on both windows and the result is averaged. The obtained phase error (and the same goes for frequency and amplitude error) is reduced significantly, in the case shown between 10 and 100 times.

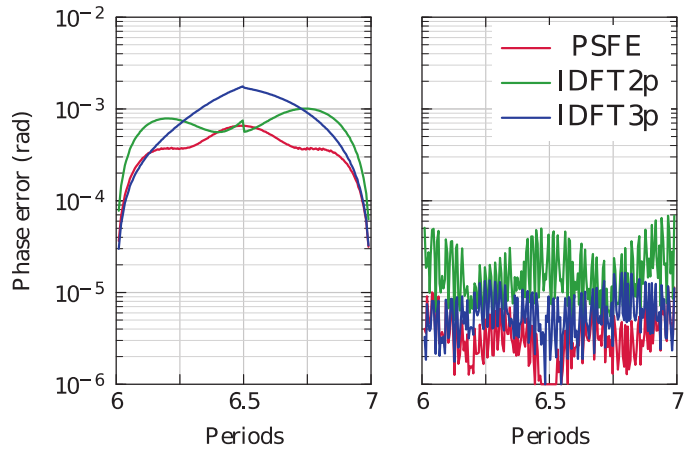


Figure 3.1: Example reduction of phase estimation error for 1 % second harmonic component in the signal.

It shall be noted that this procedure works generally on all algorithms which are insensitive to harmonic components in the coherent sampling case (this is not true for three or four parameter sine fit algorithms, which do not benefit from the developed procedure). It is equally effective for any given number of harmonic components in the signal, all the way up to the half of the Nyquist frequency. The noise performance is not compromised; in fact, it was found that for interpolated DFT algorithms, it can even be improved. The procedure requires the initial signal frequency estimation, followed by calculation of the optimal window length and finally additional two signal estimations on the windowed data. All estimations are performed using a chosen algorithm without any modifications. The processing time is approximately doubled, but inherently fast algorithms would still allow for real-time operation of improved sampled signal estimation in most practical cases.

3.3.1.2 Jitter and noise of 3458A sampling DMM modeled, measured and explained

Original Hewlett-Packard 3458A DMM (now produced by Keysight) is still a work-horse in most calibration laboratories and often found also in production facilities. It was likely one of the most often evaluated instruments and is has been produced for more than 26 years. However, its sampling jitter performance in master-slave mode and its noise performance were not fully characterised, despite they are key parameters in setting up optimal sampling scenario. The jitter performance was challenging to measure and the noise performance actually required an extremely clean signal source which was not available to date.

The jitter was successfully measured indirectly by measuring the signal to noise ratio (SNR) of single tone signal with varying frequency. It was expected that the jitter would reduce the SNR once the signal frequency would become large enough. However, it turned out that for an internal trigger that would happen beyond normal 3458A sampling bandwidth. The workaround was to use a so-called effective sampling. Using this technique and by properly compensating for the 1 μs aperture time generated roll-off, the frequency dependence of SNR was measured as shown in Figure 3.2. The SNR behaved as expected, following

$$SNR(f) = -20 \log_{10} \sqrt{\sigma_n^2 + (2\pi f t_j)^2}$$

even far over the half Nyquist frequency of 50 kHz. By fitting measured response for low frequency white noise  $\sigma_n$  and time jitter  $t_j$ , the actual sampling time jitter was estimated. For internal sampling, it was found to be below 150 ps, while for external sampling it was estimated at around 6 ns. This technique can be used universally on any ADC even over the Nyquist frequency band, provided that the used signal source noise remains constant and independent of generated signal frequency.

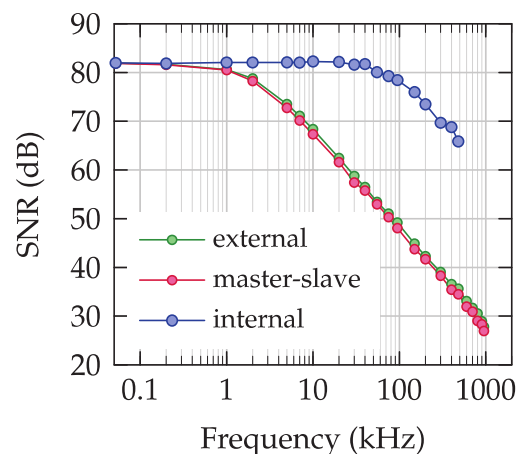


Figure 3.2: SNR frequency response shaped by a sampling jitter in different trigger modes..



This might be an issue for digitally synthesized sources, which would exhibit the same reduction of SNR due to their own time jitter.

The estimated jitter is an important parameter for sampling purposes. Statistically, it adds additional noise, which is a function of sample signal rate of change (or frequency for sine wave signal). It therefore reduces the sampling system accuracy at higher frequencies. For 3458A digital multimeter, this actually means that when using external trigger the SNR is degraded by 32 dB for full scale sine wave signal.

**3.3.1.3 Estimation of sampled arbitrary signal power**

While it is straightforward to estimate signal power for coherently sampled sinewave signals, this becomes an extremely complex problem using the same technique for arbitrary signals. Within this project, a novel technique for estimating arbitrary signal power was developed. The method is based on time domain windowing, which effectively reduces spectral leakage and thus separates the individual spectral components. Furthermore, the RMS value measurement for arbitrary waveforms using time-domain windowing was extended to power measurement, yielding an elegant and fairly effective solution to estimate arbitrary signal active power. However, the the signal cannot be completely arbitrary, as it has to fulfil the following parameters: i) the signal highest frequency has to be limited to one half of Nyquist frequency, ii) has to remain stable during the sampling acquisition and iii) its spectral components have to be separated enough between each other for the selected time-domain window function. This separation was found to be best defined in FFT bin distance. Its influence for a second tone added to the current sine wave is clearly seen in Figure 3.3. Rectangular window is the same as no window at all, showing a large and persisting error, which is effectively mitigated using in this case Hanning or Nuttall3a window. However, it was found that the estimated power standard deviation increased slightly, staying around a factor of 1.6 compared to the theoretical lower limit.

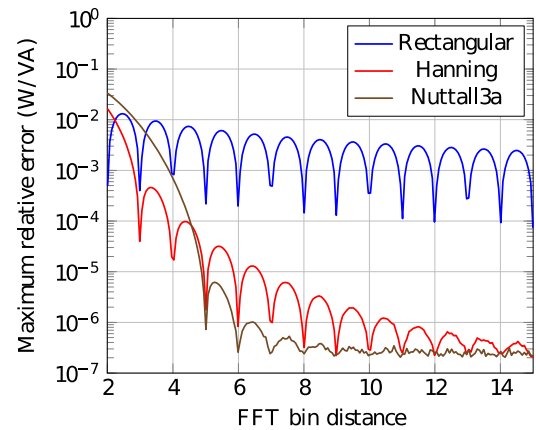


**Figure 3.3:** Maximum relative power error as a function of inter-harmonic frequency distance from the fundamental tone, given in FFT bins.

**3.3.2 Contribution of signal processing on measurement uncertainty**

Signal parameter estimation algorithms are for most cases inevitable in modern measurements incorporating signal sampling. TUBITAK, SIQ, CMI, and VSL identified error sources and their effects in digital signal generation and analogue-to-digital conversion. When the sampling is coherent, the fast Fourier transform (FFT) is commonly used to retrieve signal amplitude and phase. In this case, FFT is both unbiased and noise efficient. When coherent sampling is not possible or practical, various algorithms can be used to retrieve signal frequency, amplitude and phase with the accuracy comparable to FFT. However, only selected algorithms can fully deal with harmonic components and it becomes increasingly difficult to fully deal with interharmonic components. Additionally, the sampling noise generates random variations of the estimates and the amplitude of these variations also depends on the algorithm used. Both random variations and estimate bias need to be included in the measured parameter uncertainty budget. Bias is typically caused by signal imperfections for which the algorithm was not designed. Additionally, interpolated DFT algorithms might exhibit additional bias due to remaining spectral leakage even for clean sine wave signals when estimating parameters using a small number of sampled signal periods.

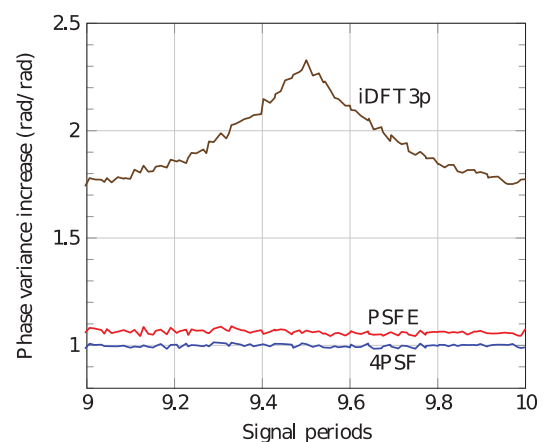


**Figure 3.4:** Noise inefficiency for three algorithm phase estimates as a function of signal periods. *iDFT3p* algorithm shows characteristic inferior performance due to processing and scalloping loss.

Random variations are limited by Cramér-Rao Lower Bound (CRLB) and better performance cannot be achieved. Some algorithms, also known as efficient algorithms, can achieve this performance (least squares based algorithms like 4PSF). However, interpolated DFT algorithms perform notably worse due to time-domain windowing processing and scalloping loss. This can increase the resulting standard deviation of estimates by a factor of 2 or even more (cf. Figure 3.4).

When an appropriate algorithm is selected for the task and the signal does not contain unwanted imperfections or these are small enough, the contribution of signal processing on measurement uncertainty can be kept small enough to be negligible. However, if this is not the case, further investigations, including numerical simulations, should be performed to assess this contributions correctly and adequately.

### 3.3.2.1 Software Toolbox

New quantum standards require new data processing techniques. Therefore in the scope of this project new signal estimation algorithms techniques have been developed (cf. sections 3.3.1.1 and 3.3.1.3). Usually for a user not specialised in data processing it takes much effort to learn how to apply a new algorithm to a measured data. Also it was found that many other useful algorithms already exist and are publically available, but they are hard to find and usually require extensive study of the documentation. To ease the adoption of the algorithms developed in this project, a quantum waveform toolbox *QWTB* was developed by CMI. The aim of the toolbox is to collect high-quality algorithms required for data processing of sampled measurements and to ease the application of the algorithms by providing unified interface and examples for every implemented algorithm, see Figure 3.5.

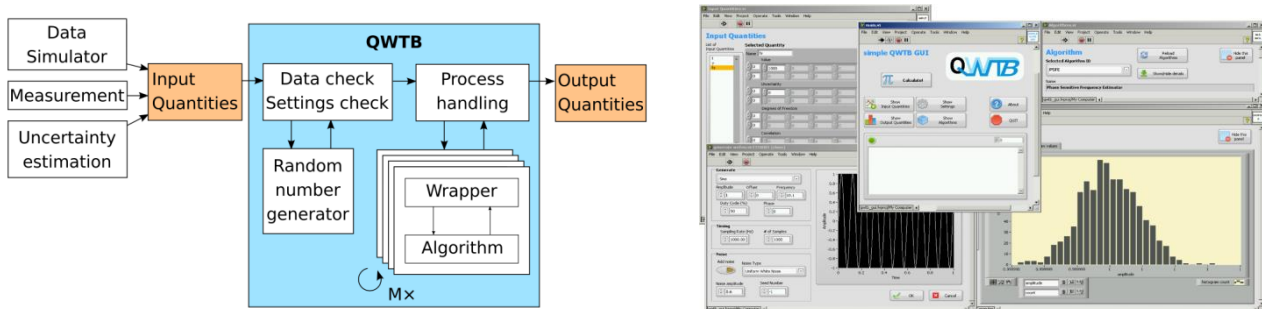


**Figure 3.5:** Left: Structure of the developed toolbox *QWTB*. User provides data in a format of generalised quantities, the toolbox reformats the data as required and handles the data to the selected algorithm. After the algorithm finish the toolbox returns output data in a format of generalized quantities. Right: Graphical user interface of the *QWTB*. User can import data, apply algorithms, review results.

*QWTB* is an open-source software toolbox written in M-code that can be run in MATLAB (commercial) or GNU Octave (open-source). The toolbox contains algorithms developed during this project and also algorithms produced in other EMRP projects (e.g. NEW04, Uncertainty: Novel mathematical and statistical approaches to uncertainty evaluation, 2012 - 2015) or developed by third-parties (details are listed in the comprehensive toolbox documentation). The user interface of the toolbox was designed to users who are not experienced in numerical computation and data processing. Some implemented algorithms can calculate propagation of uncertainties analytically. In addition, the toolbox can vary input data and calculate propagation uncertainties by means of Monte Carlo Method, however this method is very slow compared to analytical calculations. The toolbox has also a graphical user interface developed in LabVIEW (commercial). The structure of the toolbox is shown in Figure 3.5.

Thus far 15 algorithms have been implemented. Some algorithms are useful for calibrations of ADC or DAC, while others are useful for calculating calibration curves or stability estimations. Two examples of algorithms are i) *Phase Sensitive Frequency Estimator*, which is useful for fast and precise estimation of amplitude and frequency of sampled sine wave and ii) *Calibrations Curve Computing* is useful for analytical propagation of uncertainties in the case of polynomial fitting. For every algorithm an example was prepared showing a typical use case.

The toolbox itself is extensible so anyone can easily add a new algorithm. The new algorithm can be open or closed source or even a binary executable file. The license of the toolbox is very permissable and is

independent on the license of any particular algorithm. Full documentation of the toolbox, examples and instructions for adding new algorithms are available. Due to the toolbox extensibility it will be also used in ensuing EMPIR projects 15RPT04 - TracePQM and 15SIB04 - QuADC.

Because of the open source nature of the toolbox every interested party can benefit from the project results. The toolbox, its documentation and algorithms (as source code or binary according the license of the algorithm) are publicly released and available on the website <https://qwtb.github.io/qwtb/>.

A software tool used for calculating the uncertainty propagation between time and frequency domains was also developed. The GUI has multilingual interface (cf. Figure 3.6). The software reads time domain measurement results and outputs the frequency spectrum with uncertainty value. This software is feasible to process large datasets based on an approximation algorithm developed in the EMRP project IND16 Ultrafast. It is specifically optimised for low frequency application.

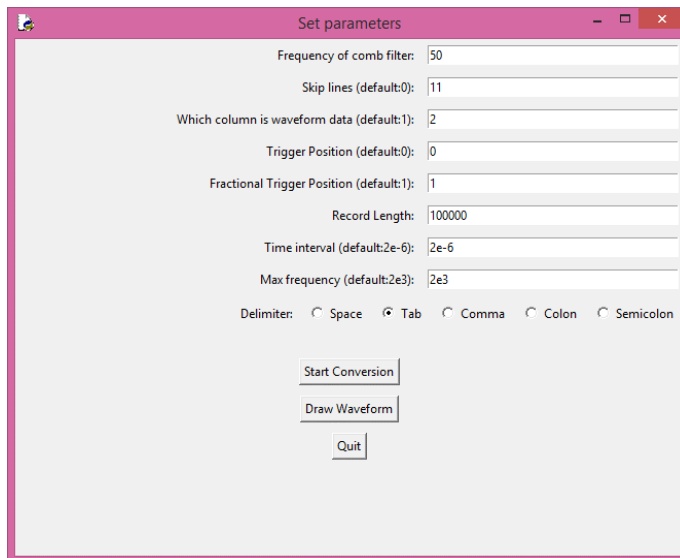


**Figure 3.6:** GUI (graphical user interface) of the uncertainty calculation tool between time and frequency domains.

### 3.3.2.2 Cable resonance phenomena for pulse-driven Josephson source explained

For high-accuracy AC-DC calibrations the DUT and the reference converter are usually connected as close as possible to each other, such that the reference plane of the measurement is close to the input connector of both DUT and reference. In this case, however, the calculable AC voltage is generated by the pulse-driven ACJVS at low temperatures (in this case 4.2 K), whereas the measurements are performed with equipment under test at room temperature, typically two meters apart. This causes the influence of the voltage leads in combination with the load and possible high frequency ground-loops to be the dominant factor in the uncertainty budget. This topic was investigated by VSL.

The project resulted in the following possible solutions:

1. The first is to use a shorter cable. The cable between probe and device under test can be as short as a few centimetres, but the length of the probe itself cannot be made much smaller than some 10 cm. One could use a cryogen-free cryostat with voltage lines of only 40-50 cm from 4.2 K to room temperature. Note that this only reduces the problem but does not solve it.
2. An alternative is to characterise the frequency behaviour and correct for it. This approach has already been used in different ways.<sup>10, 11</sup> However, for measurements at frequencies above 100 kHz, this approach is no longer valid due to the approximations made in the calculations. One assumption is that no reflections are at points other than the device under test. Furthermore, higher order terms come into play.
3. Another solution is to use impedance matching such that reflections do not occur. The input impedance of the device under test should be equal to the characteristic impedance of the voltage line between Josephson array and device under test, or a matching broadband impedance should be inserted in parallel. The problem is that the Josephson voltage source has to provide a significant amount of current, which it cannot do. Furthermore the characteristic impedance of the line is not very well known, especially at the connections to the array and when cooling down in liquid helium. The input impedance of the device under test being dependent on frequency itself will also put limitations to the success of this approach.

<sup>10</sup> P.S. Filipski, M. Boecker, S.P. Benz, C.J. Burroughs, *Experimental determination of the voltage lead error in an ac Josephson voltage standard*, IEEE Trans. Instrum. Meas. **60** (2011) 2387–2392.

<sup>11</sup> H.E. van den Brom and E. Houtzager, *Voltage lead corrections for a pulse driven ac Josephson voltage standard*, Meas. Sci. Technol. **23** (2012) 124007 (7pp).

A combination of 1 and 2 gives reliable results at frequencies up to 100 kHz, but not above. Solution 3 might work at higher frequencies but has limited applicability. Further research is necessary to find an optimal solution.

### 3.3.3 Characterisation of converters

The aim of work was the identification of metrology grade ADC parameters that require improved characterisation techniques from those already described by available standards, and the preparation of a proposal for the inclusion of new test methods in these standards. For identified parameters, new calibration and test procedures were developed and a proposal was submitted for their inclusion in current ADC and DAC standards.

#### 3.3.3.1 List of analogue-to-digital converter parameters that require improved characterisation

The IEEE Standard “Terminology and Test Methods for Analog-to-Digital Converters (IEEE Std 1241-2010)” provides one of the most available complete description for the characterisation of Analogue-to-Digital Converters (ADC) but some improvements were required. The main necessary improvements are the use of traceable references to the SI and the uncertainty estimation. In this project, new parameters as time aperture gain dependence and temperature and humidity influence were defined. The result of the revision was presented and discussed by CEM at the Spanish national standard committee (AENOR, CTN-82).

#### 3.3.3.2 High accuracy parameters that require improved characterisation

As in most cases the uncertainty estimation of all parameter determinations is very complex, the work required to prepare a procedure with the necessary improvements was not feasible to be completely afforded in this project. Besides, the amount of necessary changes requires working in a step by step way. The final decision was to work on a selected parameter, the frequency response of the ADCs because this characterisation will use most of the achievements of the project. The new references and a first draft of the measurement procedure have been prepared.

#### 3.3.3.3 Procedure for improved characterisation of ADC

The aim of this procedure was the calibration of the frequency response of ADCs. The procedure, which can be used for the characterisation of any ADC, is particularised for the characterisation of the frequency response of the DCV function of a Keysight 3458 Digital Multimeter. The frequency characterisation is performed on the 1 V range applying 0.8 V RMS signal at frequencies up to 20 kHz.

The method is based on comparing the known input signal to the values obtained sampling the input signal using the DCV digitizing function of a 3458 Digital Multimeter. The reference was a calibrated, dual sine wave generator (DualDAC 2) for metrological applications at low frequencies (0.1 Hz - 20 kHz) developed within this project. The source was calibrated with a true quantum based source. Stability and performance of the source has been verified by means of an inter-comparison within several project partners. For each frequency, the calibrated AC source ( $U(f)$ ) was applied to the ADC at some defined operation conditions. The estimate of the output signal ( $A(f)$ ) was obtained from the taken samples using a convenient algorithm.

The processing of the samples can be performed using the toolbox *QWTB* or any other applications. The file containing samples is read as the input of the processing stage. Other information may be required depending on the selected processing method. If FFT is used, a sampling rate needs to be provided as an input via a measurement configuration file. With this information, the spectral analysis of the samples

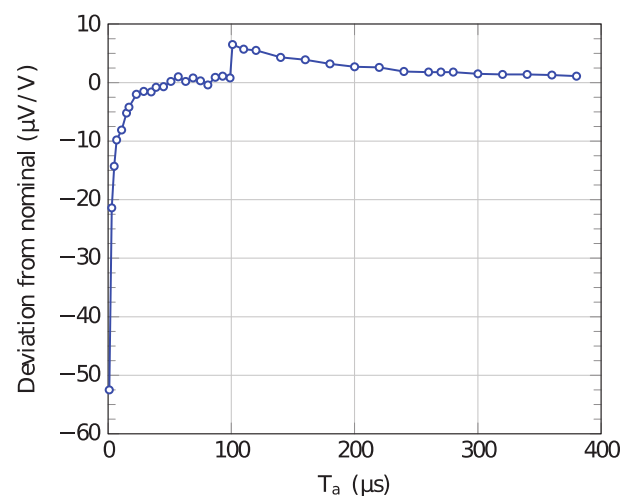


**Figure 3.7:** Gain variation of a Keysight 3458A type sampling voltmeter as a function of aperture time  $T_a$ .



is performed by (windowed) FFT. If least squares sine wave method is used, the signal frequency estimation is needed to obtain best results.

The uncertainty estimation is performed according to the “Guide to the expression of uncertainty in measurement” and will be mainly based on Supplement 1 “Guide to the expression of uncertainty in measurements (GUM) – propagation of distributions using a Monte Carlo method”. Calculations can be performed using the Software toolbox specifically developed within this project or any other appropriate application.

The procedure has been tested with practical characterisations of a Keysight 3458. The time aperture gain dependence needed to be estimated in order to apply a correction especially when there is a signal frequency low time aperture and also for the uncertainty estimation. Figure 3.7 shows the gain variations obtained for different  $T_a$  applying a sine wave signal 0.8 V and 53 Hz. Similar behaviour has been obtained at different frequencies.

### 3.3.4 Conclusion

In this project digital signal processing techniques and their contribution to the measurement uncertainty were evaluated and improved. Key achievements beyond existing procedures were the development of:

- Sampled signal estimation for harmonically distorted signals improved;
- Jitter and noise of 3458A sampling DMM modeled, measured and explained;
- Cable resonance phenomena for pulse-driven Josephson source explained;
- Quantum Waveform ToolBox *QWTB* developed;
- ADC parameters that require improved characterisation listed;
- Procedure for improved characterisation of ADCs developed.

In conclusion, the estimation of harmonically distorted fundamental signal parameters was greatly improved, reducing sensitivity to harmonic components by a factor of ten to one hundred. Jitter and noise of the 3458A sampling DMM was modeled, measured and explained. Calculations concerning waveforms above 100 kHz synthesised by pulse-driven Josephson arrays revealed that the cause of the problem should not be thought of as a resonance, but as the start of a standing wave phenomena. Further investigations confirmed the predicted squared amplitude dependence on frequency and cable length. A Quantum Waveform ToolBox *QWTB* developed collects high-quality algorithms required for data processing of sampled measurements and makes the application of the algorithms easier by providing a unified interface and examples for every implemented algorithm. The toolbox is open source and can be extended with additional algorithms by each user.

## 4 Actual and potential impact

This research project has been set in the context of the *EMRP Outline 2008*, section I.1.2.2, “Focussed single discipline and applied metrology” which refers to advanced realisations of derived SI units and applied metrology to support innovation, products and services. Within the SI it has been directed at the provision of “intrinsically referenced standards” by exploiting the quantum standard of voltage, in the form of the Josephson effect, to provide direct traceability for dynamically varying or AC voltages. In this way it has been aimed specifically at broadening the scope of the SI to provide quantum traceability for non-stationary voltages for the first time, especially for arbitrary waveforms for which there has had been no direct route at all. Then, electrical quantum metrology has been applied to the growing use of digital metrology whereby electrical currents and voltages from sensors are converted to numerical values for further processing and analysis. The use of digital techniques is at the heart of most modern instrumentation products and innovation in this sector depends on new methods for disseminating the SI volt for sampled electrical measurements.

The project resulted in new capabilities for the provision of traceability for sampled electrical measurements directly to the SI using voltage references based on the Josephson effect. The sections below describe the activities related to actual and potential impact of the project achievements.



#### 4.1 Dissemination of results

11 peer-reviewed publications have been submitted, from which 10 are already published; in addition, 29 peer-reviewed proceedings have been published. The project partners gave 55 presentations at national and international conferences and 19 presentations at workshops. 4 good practice guides are also available on the project website:

- Practical advice on building an active filter for Delta-Sigma modulated Josephson waveforms
- Characterisation of ADCs in the time and frequency domains using a Programmable Josephson Voltage Standard
- Good Practice Guide: The DualDAC2
- Proper operation of the AC reference standard

Newsletters were sent to the stakeholders and stakeholder workshops based on outcomes of the project covered: (i) the AC quantum voltmeter, (ii) the pulse-driven AC Josephson voltage standard, and the combined system consisting of the PJVS and the pulse-driven AC Josephson voltage standard.

A unique QWTB was developed containing algorithms for the evaluation of generators and digitisers errors. The QWTB significantly improves precision measurements using sampling methods and evaluating their uncertainties especially for operators without high-level metrological expertise. The QWTB, its documentation and algorithms are publicly available from the project website <https://qwtb.github.io/qwtb/>.

The final dissemination meeting was held in conjunction with the EMRP projects SIB51 'GraphOhm' and SIB53 'AIM QuTE'. This combined meeting attracted more than 55 of the main European experts from the field of voltage, impedance and quantum metrology and their metrological application, including representatives from European metrology bodies, and international experts from countries such as Korea, Japan and USA.

#### 4.2 Impact on the metrological and scientific communities

This project supported the implementation of capabilities and methodologies to realise sampling methods. In particular, a step change is expected from time consuming measurements based on AC-DC transfer to fast and precise sampling methods giving the full information of a waveform. The major impact will be improved knowledge for precision measurements using sampling methods.

As part of a Researcher Mobility Grant (RMG) from TUBITAK identified and quantified the major error sources of the combined PJVS and AC Josephson Voltage Standard system by connecting theoretical uncertainty studies and practical investigation.

Outcomes from this project have already been used in the EMPIR projects 14RPT01 ACQ-PRO *Towards the propagation of ac quantum voltage standards* and 15SIB04 QuADC *Waveform metrology based on spectrally pure Josephson voltages*, which also relate Josephson voltage standards and high-precision voltage measurements.

The outputs of this project will also improve calibration and measurement services at the NMI level. This includes fast waveform measurements and also measurements of arbitrary waveforms. For example, the first comparison loop on arbitrary waveforms was performed with 4 NMIs and so far the results are preliminary, but it is already clear that sampling method results are as good as results achieved with existing AC-DC transfer standards. In the longer term NMIs can disseminate waveform calibration results based on calculations using the QWTB. An important exploitation area is expected to be consultancy and advice on the calibration of arbitrary waveform instrumentation to industry.



#### **4.3 Impact on standardisation**

The project participated in EURAMET Technical Committee for Electro Magnetism (TC-EM) and the Spanish national standards body AENOR Metrology & Calibration CTN-82, as well as informing the EURAMET DC and Quantum Metrology working group.

Metrology grade ADC parameters were investigated by the project, in order to identify those parameters that require improved characterisation techniques. It was established that the use of traceable references to the SI and the uncertainty estimation require improvements. In addition, new parameters as time aperture gain dependence and temperature and humidity influence were defined. These results were presented and discussed by CEM at AENOR, CTN-82.

#### **4.4 Early impact on end users**

The project has already had an impact on calibration services and instrument manufacturers who are interested in the DualDAC2 instrument commercially available from AIVON Ltd (considered to be the superior tool for highly precise traceable generation of arbitrary waveforms). With its excellent features, the DualDAC2 sets new benchmarks, and is expected to become a new cornerstone in metrology and calibration applications dealing with arbitrary waveforms, used by NMIs, high-level calibration labs, manufactures of high-precision instrumentation.

The unique QWTB containing algorithms for evaluation of generators and digitisers errors, its documentation and algorithms are publicly available from the project website. These are relevant for high-precision measurements, so the main users will be from NMIs, high-level calibration labs, and research institutes.

#### **4.5 Potential future impact**

This project was centred on the measurement of waveforms used in digital electronics. The uptake of the new measurement capabilities available at NMIs by the calibration and instrumentation sector will over time lead to longer-term economic, environmental and social impact.

Economic impact will be created via technology developments in electronics and modern ADCs and DACs. The sensor industry represents a multi-billion Euro market and errors in testing can cause additional expenses to manufacturers of high-volume electronic devices.

The long-term impact for the environmental and health sector will be through improved designs of ADC and DAC components and systems that will help to increase performance and reduce measurement time. Characterisation is a significant part of the overall cost of manufacturing, and thus a reduction in this through more efficient testing will lead to lower prices and wider adoption of precision devices.



## 5 Website address and contact details

The address of the project public website:

[www.ptb.de/emrp/qwave.html](http://www.ptb.de/emrp/qwave.html)

The address of the project coordinator:

Dr. Johannes Kohlmann  
 Physikalisch-Technische Bundesanstalt (PTB)  
 Bundesallee 100  
 38116 Braunschweig  
 Germany

Phone: + 49 (0) 531 592 2133

E-Mail: [johannes.kohlmann@ptb.de](mailto:johannes.kohlmann@ptb.de)

## 6 List of publications

### Peer-reviewed publications (status: 31 October 2016):

- [1] O. F. Kieler, R. Behr, R. Wendisch, S. Bauer, L. Palafox, J. Kohlmann, *Towards a 1 V Josephson Arbitrary Waveform Synthesizer*, IEEE Trans. Appl. Supercond. **25** (2015) 1400305 (5 pp.).
- [2] O.F.O. Kieler, T. Scheller, J. Kohlmann, *Cryocooler operation of a pulse-driven AC Josephson voltage standard at PTB*, World J. Condens. Matter Phys. **3** (2013) 189–193.
- [3] B. Jeanneret, F. Overney, C. Scherly, G. Schaller, *Josephson-based characterization of analog-to-digital converters using an equivalent time sampling method*, CPEM 2016 Conference Digest (2016) doi: 10.1109/CPEM.2016.7540767.
- [4] R. Behr, O. Kieler, J. Lee, S. Bauer, L. Palafox, J. Kohlmann, *Direct comparison of a 1 V Josephson arbitrary waveform synthesizer and an ac quantum voltmeter*, Metrologia **52** (2015) 528–537.
- [5] H.E. van den Brom, Dongsheng Zhao, E. Houtzager, *Voltage lead errors in an AC Josephson voltage standard: explanation in terms of standing waves*, CPEM 2016 Conference Digest (2016) doi: 10.1109/CPEM.2016.7540666.
- [6] H.E. van den Brom, O.F.O. Kieler, S. Bauer, E. Houtzager, *AC-DC Calibrations with a pulse-driven AC Josephson voltage standard operated in a small cryostat*, CPEM 2016 Conference Digest (2016) doi: 10.1109/CPEM.2016.7540605.
- [7] A. Sosso, N. De Leo, M. Fretto, E. Monticone, L. Roncaglione, R. Rocci, V. Lacquaniti, *Cryocooler operation of SNIS Josephson arrays for AC voltage standards*, J. Phys.: Conf. Ser. **507** (2014) 042040 (4pp).
- [8] J. Díaz de Aguilar, M. Anguas, Y.A. Sanmamed, R. Caballero, K. Schweiger, M. Neira, *Los convertidores digitales como futuro patrón corriente alterna. El proyecto europeo "Q-Wave"*, 5<sup>th</sup> Congreso Español de Metrología 2013, Conference Digest (2013) paper 23P2T (7 pp), in Spain.
- [9] R. Lapuh, B. Voljč, M. Kokalj, B. Pinter, Z. Svetik, M. Lindič, *Measurement of repetitive arbitrary waveform RMS value*, CEPM 2014 Conference Digest (2014) 420–421.
- [10] J.R. Salinas, J. Díaz de Aguilar, F. Garcia-Lagos, G. Joya, F. Sandoval, M. L. Romero, *Spectrum analysis of asynchronously sampled signals by means of an ANN method*, CEPM 2014 Conference Digest (2014) 422–423.
- [11] T. Bergsten, G. Eklund, V. Tarasso, K.-E. Rydler, *An active filter for Delta-Sigma modulated Josephson waveforms*, CPEM 2014 Conference Digest (2014) 518–519.
- [12] B. Trinchera, A. Sosso, U. Pogliano, V. Lacquaniti, E. Monticone, M. Fretto, R. Rocci, L. Roncaglione Tet, D. Serazio, *Wideband digital modular system for dynamic characterization of PJVS*, CPEM 2014 Conference Digest (2014) 114–115.



- [13] J. Ireland, D. Henderson, J. Williams, O. Kieler, J. Kohlmann, R. Behr, J. Gran, H. Malmbekk, K. Lind, Chi Kwong Tang, *An opto-electronic coupling for pulse-driven Josephson junction arrays*, CPEM 2014 Conference Digest (2014) 124–125.
- [14] J. Gran, H. Malmbekk, K. Lind, *Photodiodes as current source in high-frequency low temperature applications*, CPEM 2014 Conference Digest (2014) 266–267.
- [15] M. Šíra, S. Mašláň, *Uncertainty analysis of non-coherent sampling phase meter with four parameter sine wave fitting by means of MonteCarlo*, CPEM 2014 Conference Digest (2014) 334–335.
- [16] R. Behr, O. Kieler, S. Bauer, L. Palafox, J. Kohlmann, *Development of a 1 V pulse-driven Josephson voltage standard*, CPEM 2014 Conference Digest (2014) 418–419.
- [17] J. Kohlmann, F. Müller, O. Kieler, T. Scheller, B. Egeling, R. Wendisch, R. Behr, *Josephson series arrays with NbSi barrier for AC voltage standards*, CPEM 2014 Conference Digest (2014) 466–467.
- [18] J. Kohlmann, R. Behr, O. Kieler, J. Diaz de Aguilar, M. Šíra, A. Sosso, B. Trinchera, J. Gran, H. Malmbekk, B. Jeanneret, F. Overney, J. Nissila, T. Lehtonen, J. Ireland, J. Williams, R. Lapuh, B. Voljc, T. Bergsten, G. Eklund, T. Coskun Öztürk, E. Houtzager, H.E. van den Brom, P. Ohlckers, *A quantum standard for sampled electrical measurements – main goals and first results of the EMRP project Q-WAVE*, CPEM 2014 Conference Digest (2014) 522–523.
- [19] A. Sosso, B. Trinchera, E. Monticone, M. Fretto, R. Rocci, L. Roncaglione, D. Serazio, V. Lacquaniti, *Operation of SNIS arrays in a cryocooler*, CPEM 2014 Conference Digest (2014) 658–659.
- [20] J. Lee, J. Nissilä, A. Katkov, R. Behr, *A quantum voltmeter for precision AC measurements*, CPEM 2014 Conference Digest (2014) 732–733.
- [21] T.C. Öztürk, J. Kohlmann, O. Kieler, T. Möhring, R. Behr, H. Çaycı, M. Arifoviç, S. Turhan, L.D. Ata, *Error analysis in waveforms with a combined Josephson system for AC component characterization*, CPEM 2014 Conference Digest (2014) 734–735.
- [22] M. Šíra, S. Mašláň, V. Nováková Zachovalová, *Design, stability analysis and uncertainty contribution of a voltage divider designed for a phase meter*, 20th IMEKO TC4 International Symposium and 18th IMEKO TC-4 International Workshop on ADC and DAC Modelling and Testing, Conference Digest (2014) 942–946.
- [23] R. Lapuh, B. Voljč, M. Lindič, *Evaluation of Agilent 3458A Time Jitter Performance*, IEEE Trans. Instrum. Meas. **64** (2015) 1331–1335.
- [24] T. Bergsten, G. Eklund, V. Tarasso, K.-E. Rydler, *An active filter for Delta–Sigma-modulated Josephson waveforms*, IEEE Trans. Instrum. Meas. **64** (2015) 1559–1563.
- [25] E. Bardalen, M. Nadeem Akram, H. Malmbekk, P. Ohlckers, *Review of Devices, Packaging, and Materials for Cryogenic Optoelectronics*, Journal of Microelectronics and Electronic Packaging **12** (2015) 189–204.
- [26] J. Kohlmann, O. Kieler, T. Scheller, B. Egeling, R. Wendisch, R. Behr, *Series arrays of NbSi barrier Josephson junctions for AC voltage standards*, CPEM 2016 Conference Digest (2016) doi: 10.1109/CPEM.2016.7540562.
- [27] J. Diaz de Aguilar, J.R. Salinas, R. Lapuh, A. Méndez, F. Garcia Lagos, Y.A. Sanmamed, *Characterization of the frequency response of Analog-to-Digital Converters*, CPEM 2016 Conference Digest (2016) doi: 10.1109/CPEM.2016.7540455.
- [28] J.R. Salinas, F. García-Lagos, Javier Díaz de Aguilar, G. Joya, R. Lapuh, F. Sandoval, *Harmonics and interharmonics spectral analysis by ANN*, CPEM 2016 Conference Digest (2016) doi: 10.1109/CPEM.2016.7540649.
- [29] M. Šíra, S. Mašláň, V. Nováková Zachovalová, *QWTB – Software Tool Box for Sampling Measurements*, CPEM 2016 Conference Digest (2016) doi: 10.1109/CPEM.2016.7540599.
- [30] R. Lapuh, B. Voljč, M. Lindič, *Measurement and estimation of arbitrary signal power using a window technique*, CPEM 2016 Conference Digest (2016) doi: 10.1109/CPEM.2016.7540739.



- [31] R. Lapuh, B. Voljč, M. Kokalj, M. Lindič, Z. Svetik, *Quasi coherent overlapping procedure to improve harmonics suppression using single tone estimation algorithms*, CPEM 2016 Conference Digest (2016) doi: 10.1109/CPEM.2016.7540596.
- [32] R. Lapuh, M. Šira, M. Lindič, B. Voljč, *Uncertainty of the Signal Parameter Estimation from Sampled Data*, CPEM 2016 Conference Digest (2016) doi: 10.1109/CPEM.2016.7540770.
- [33] R. Lapuh, B. Voljč, M. Lindič, *Keysight 3458A Noise Performance*, CPEM 2016 Conference Digest (2016) doi: 10.1109/CPEM.2016.7540597.
- [34] J. Ireland, A. Cryer, J.M. Williams, E. Houtzager, R. Hornecker, H.E. van den Brom, *Design of delta-sigma feedback loop for quantum voltage digitizer*, CPEM 2016 Conference Digest (2016) doi: 10.1109/CPEM.2016.7540457.
- [35] E. Bardalen, Thai Anh Tuan Nguyen, H. Malmbekk, O. Kieler, P. Ohlckers, *Packaging of fiber-coupled module for Josephson junction array voltage standards*, CPEM 2016 Conference Digest (2016) doi: 10.1109/CPEM.2016.7540561.
- [36] A. Sosso, B. Trinchera, P. Durandetto, E. Monticone, O. Kieler, R. Behr, J. Kohlmann, *Tests on waveform synthesis in a new cryocooler setup*, CPEM 2016 Conference Digest (2016) doi: 10.1109/CPEM.2016.7540563.
- [37] L. Palafox, R. Behr, O. Kieler, J. Lee, I. Budovsky, S. Bauer, T. Hagen, *First metrological applications of the PTB 1 V Josephson Arbitrary Waveform Synthesizer*, CPEM 2016 Conference Digest (2016) doi: 10.1109/CPEM.2016.7540602.
- [38] J. Nissila, M. Sira, J. Lee, T. Öztürk, M. Arifovicm J. Diaz de Aguilar, R. Lapuh, R. Behr, *Stable arbitrary waveform generator as a transfer standard for ADC calibration*, CPEM 2016 Conference Digest (2016) doi: 10.1109/CPEM.2016.7540454.
- [39] A. Sosso, P. Durandetto, B. Trinchera, O. Kieler, R. Behr, J. Kohlmann, *Characterization of a Josephson array for pulse-driven voltage standard in a cryocooler*, *Measurement* **95** (2017) 77–81.

### Good Practice Guides

- [G1] T. Bergsten, *Good Practice Guide: Practical advice on building an active filter for Delta-Sigma modulated Josephson waveforms*, JRP SIB59 Q-WAVE, July 2015.
- [G2] J. Nissila, *Good Practice Guide: The DualDAC2*, JRP SIB59 Q-WAVE, January 2016.
- [G3] B. Trinchera, A. Sosso, *Good Practice Guide: Proper operation of the AC reference standard developed by INRIM / TUBITAK*, JRP SIB59 Q-WAVE, January 2016.
- [G4] B. Jeanneret, *Good Practice Guide: Characterisation of ADCs in the time and frequency domains using a Programmable Josephson Voltage Standard*, JRP SIB59 Q-WAVE, April 2016.